

Pharmacology of Indole and Indazole Synthetic Cannabinoid Designer Drugs AB-FUBINACA, ADB-FUBINACA, AB-PINACA, ADB-PINACA, 5F-AB-PINACA, 5F-ADB-PINACA, ADBICA, and 5F-ADBICA

Samuel D. Banister,^{†,‡} Michael Moir,[‡] Jordyn Stuart,[§] Richard C. Kevin,^{||} Katie E. Wood,^{||} Mitchell Longworth,[‡] Shane M. Wilkinson,[‡] Corinne Beinat,^{†,‡} Alexandra S. Buchanan,^{⊥,#} Michelle Glass,[○] Mark Connor,[§] Iain S. McGregor,^{||} and Michael Kassiou^{*,‡,∇}

[†]Department of Radiology, [⊥]Center for Immersive and Simulation-Based Learning, Stanford University School of Medicine, Stanford, California 94305, United States

[‡]School of Chemistry, ^{||}School of Psychology, [∇]Faculty of Health Sciences, The University of Sydney, Sydney, NSW 2006, Australia

[§]Faculty of Medicine and Health Sciences, Macquarie University, Sydney, NSW 2109, Australia

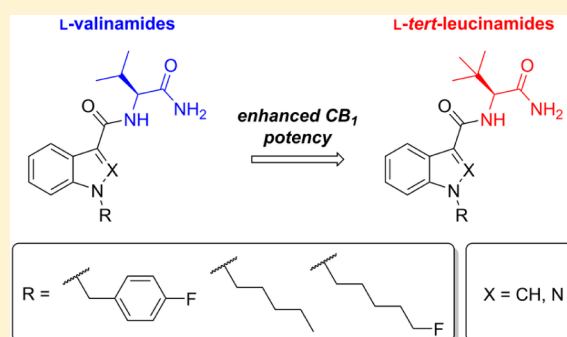
[#]Department of Anaesthesia, Prince of Wales Hospital, Randwick, NSW 2031, Australia

[○]School of Medical Sciences, The University of Auckland, Auckland 1142, New Zealand

Supporting Information

ABSTRACT: Synthetic cannabinoid (SC) designer drugs based on indole and indazole scaffolds and featuring *L*-valinamide or *L*-tert-leucinamide side chains are encountered with increasing frequency by forensic researchers and law enforcement agencies and are associated with serious adverse health effects. However, many of these novel SCs are unprecedented in the scientific literature at the time of their discovery, and little is known of their pharmacology. Here, we report the synthesis and pharmacological characterization of AB-FUBINACA, ADB-FUBINACA, AB-PINACA, ADB-PINACA, 5F-AB-PINACA, 5F-ADB-PINACA, ADBICA, 5F-ADBICA, and several analogues. All synthesized SCs acted as high potency agonists of CB₁ (EC₅₀ = 0.24–21 nM) and CB₂ (EC₅₀ = 0.88–15 nM) receptors in a fluorometric assay of membrane potential, with 5F-ADB-PINACA showing the greatest potency at CB₁ receptors. The cannabimimetic activities of AB-FUBINACA and AB-PINACA *in vivo* were evaluated in rats using biotelemetry. AB-FUBINACA and AB-PINACA dose-dependently induced hypothermia and bradycardia at doses of 0.3–3 mg/kg, and hypothermia was reversed by pretreatment with a CB₁ (but not CB₂) antagonist, indicating that these SCs are cannabimimetic *in vivo*, consistent with anecdotal reports of psychoactivity in humans.

KEYWORDS: Cannabinoid, THC, JWH-018, FUBINACA, PINACA



Synthetic cannabinoids (SCs) are the most rapidly growing class of recreational designer drugs. Since the identification of the first SC designer drugs in 2008, more than 130 SCs have been reported to the European Monitoring Centre for Drugs and Drug Addiction (EMCDDA).¹ Of the 101 new psychoactive substances notified by the EMCDDA during 2014, 30 were SCs.¹ Although these products are often mislabeled as research chemicals or incense and include disclaimers stating that the products are not for human consumption, SCs are recreational designer drugs intended to mimic the effects of Δ^9 -tetrahydrocannabinol (Δ^9 -THC, **1**, Figure 1) while circumventing the law.

The phytocannabinoid Δ^9 -THC is the principal bioactive component of marijuana (*Cannabis sativa*), the most widely used illicit substance in the world. Δ^9 -THC exerts its psychoactive effects by acting as a partial agonist at cannabinoid type-1 (CB₁) receptors,² although it is also a partial agonist at

type-2 (CB₂) receptors. CB₁ and CB₂ receptors are classical G protein-coupled receptors (GPCRs). While CB₁ receptors are found primarily at the terminals of central and peripheral neurons, where they inhibit neurotransmitter release, CB₂ receptors are mainly located in immune cells within and outside the central nervous system (CNS).^{3,4} Due to the role of the CB receptor system in numerous diseases, early pharmaceutical drug discovery programs explored many phytocannabinoid analogues like CP 47,497 (**2**) and CP 55,940 (**3**), disclosed by Pfizer in the 1970s and 1980s.^{5,6} Following structural leads from the pharmaceutical industry, Huffman and co-workers at Clemson University have

Received: April 8, 2015

Revised: June 9, 2015

Published: July 2, 2015

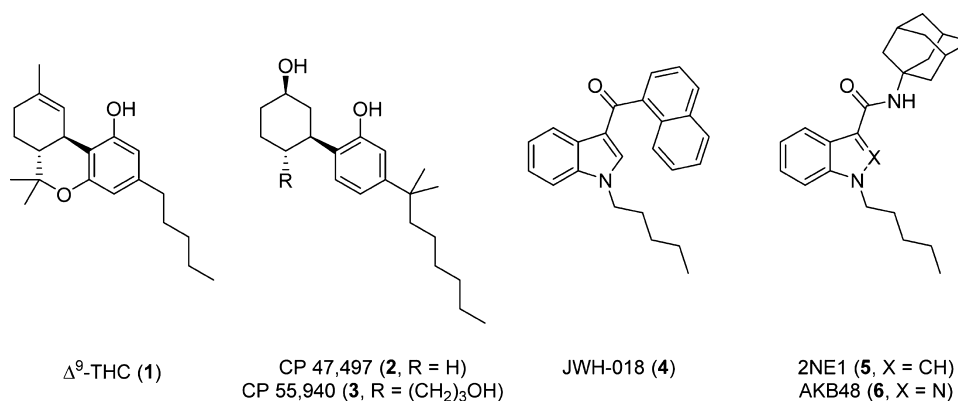


Figure 1. Selected phytocannabinoids and synthetic cannabinoids.

discovered many indole SCs with potent cannabimimetic activity, including JWH-018 (4).

In 2008, a recreational herbal blend was found to contain the C8 homologue of CP 47,497 and JWH-018.⁷ Following the prohibition of CP 47,497-C8 and JWH-018 by many governments, other structurally diverse indole SCs began to appear.^{8–11} Recently, numerous SCs with clandestine design origins and no precedent in the scientific literature have been detected in forensic samples. For example, indole-3-carboxamide SC 2NE1 (APICA, SDB-001, 5) was identified along with its indazole analogue AKB48 (APINACA, 6).¹² Presumably intended to mimic the alphanumeric format of compound codes used throughout the pharmaceutical industry, 2NE1 and AKB48 were named after Japanese and Korean female pop music groups, respectively, by their clandestine designers. Current popular design trends for modification of the *N*-pentyl group include terminal fluorination and replacement with cyclohexylmethyl or 4-fluorobenzyl moieties.^{13,14}

In 2013, novel indazole SCs AB-FUBINACA (7, Figure 2) and ADB-FUBINACA (8) were identified in recreational products by Japanese forensic scientists.^{10,15,16} Although many recent SCs have no precedent in the scientific literature prior to their identification as designer drugs, 7 and 8 were both described by Pfizer in a 2009 patent claiming CB₁ ligands as potential therapeutic agents.¹⁷ The binding affinity and functional activity in a GTP γ S binding assay of 7 (K_i = 0.9 nM, EC_{50} = 23.2 nM) and 8 (K_i = 0.36 nM, EC_{50} = 0.98 nM) at hCB₁ receptors was reported, indicating that both compounds are potent CB₁ agonists, but no further pharmacology was described. The stereochemistry of the isopropyl and *tert*-butyl side chains of illicit 7 and 8, respectively, is unresolved. However, the Pfizer patent reports activity exclusively for the (*S*)-enantiomers, and it is likely that the Pfizer compounds and the illicit SCs are (*S*)-enantiomers derived from the abundant and inexpensive *L*-amino acids *L*-valine and *L*-*tert*-leucine.

AB-PINACA (9) was identified alongside 7, representing a hybrid of 7 and *N*-pentyl SCs like 4 and 6.^{10,15} Although previously unreported in the scientific literature, ADB-PINACA (10) exposure was associated with severe adverse reactions, including neurotoxicity and cardiotoxicity in the USA in late 2013,^{18–20} and was recently linked to a cluster of cases of severe delirium.²¹ The 5-fluorinated analogues of 9 and 10, 5F-AB-PINACA (11) and 5F-ADB-PINACA (12), respectively, have also been identified on the Japanese market.^{22,23} By 2014, 7–11 and 16 had been formally notified by the EMCDDA as a result of seizures in Belgium, Germany, Turkey, the United Kingdom, and Sweden.²⁴

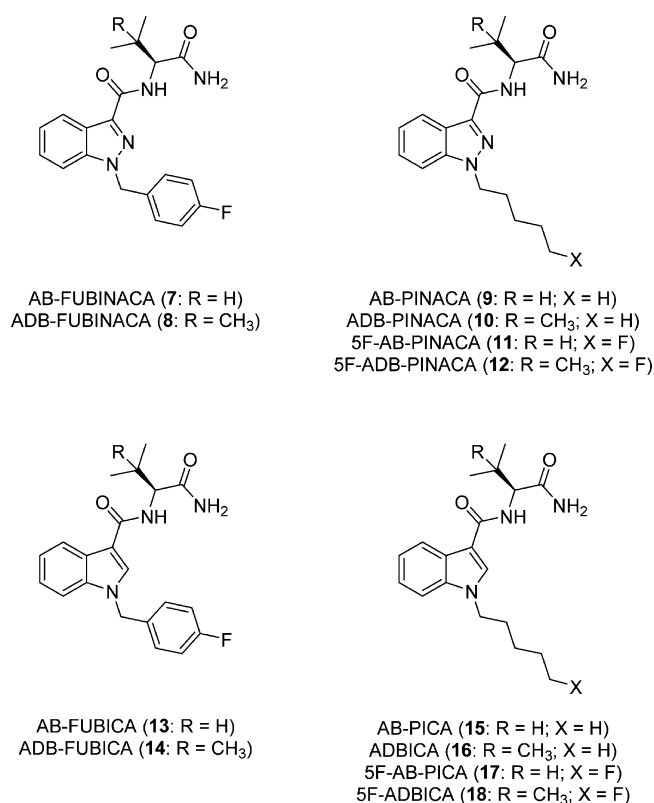


Figure 2. Indole- and indazole-3-carboxamide synthetic cannabinoid designer drugs.

AB-FUBICA (13), ADB-FUBICA (14), AB-PICA (15), and 5F-AB-PICA (17) represent the indole analogues of indazoles 7, 8, 9, and 11 and have not appeared in the scientific literature. However, the indole analogue of 10, ADBICA (16) was identified in Japan,¹⁶ and its 5-fluoro analogue, 5F-ADBICA (18), was notified by the EMCDDA after law enforcement agencies in the U.S. implicated 18 in a series of non-fatal intoxications.²⁴

Despite their widespread use and frequency of adverse reactions requiring hospitalization, very little is known about the activity of indole and indazole SCs comprising an *L*-valinamide or *L*-*tert*-leucinamide subunit. In addition to reports of the detection of SCs 7–11, 16, and 18 by forensic researchers, the metabolic profiles of 7–9 and 11 were recently published.^{25–28}

The aim of the present study was to address the paucity of data regarding the pharmacology of indole and indazole SCs by synthesizing 7–18, evaluating their activity at human CB₁ and CB₂ receptors, and assessing the behavioral pharmacology of these novel SCs in rats using biotelemetry.

RESULTS AND DISCUSSION

The original patent by Pfizer describing AB-FUBINACA and ADB-FUBINACA utilized enantiopure amino acids *L*-valinamide (19, Figure 3) and *L*-*tert*-leucinamide (20) to give products with (*S*) stereocenters.

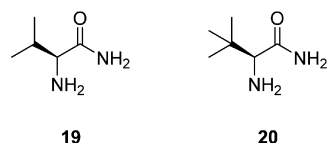


Figure 3. Amino acid derivatives *L*-valinamide (19) and *L*-*tert*-leucinamide (20).

While *L*-valinamide is available from numerous commercial sources as its hydrochloride salt, *L*-*tert*-leucinamide is derived from a non-natural amino acid, and the synthesis of 20 is shown in Scheme 1. Treatment of *L*-*tert*-leucine (21) with benzyl chloroformate gave Cbz-protected amine 22. The free acid of 22 was converted to the corresponding amide (23) using the coupling reagents EDC and HOBt, and subsequent deprotection by catalytic hydrogenation afforded 20. The three-step procedure proved to be operationally convenient, and analytically pure *L*-*tert*-leucinamide was obtained on a multigram scale following recrystallization.

The synthesis of indazole SCs 7–12 is shown in Scheme 2. Fischer esterification of indazole-3-carboxylic acid (24) gave 25, which was deprotonated with potassium *tert*-butoxide and alkylated with either 4-fluorobenzyl bromide, 1-bromopentane, or 1-bromo-5-fluoropentane to afford the corresponding *N*-alkylindazole-3-carboxylic acid methyl esters 26–28. Alkylation proceeded regioselectively to give 1-substituted 1*H*-indazoles as the major products; however, small quantities of 2-alkylated indazoles were obtained as minor products and separated by flash chromatography. Saponification of the methyl ester of 26–28 to give free acids 29–31 was followed by amide coupling with EDC-HOBt and either *L*-valinamide or *L*-*tert*-leucinamide to give 7–12.

Access to the corresponding indole SCs (13–18) required an alternative synthetic route, shown in Scheme 3. Excess sodium hydride was added to indole (33), which was subsequently alkylated with the appropriate bromoalkane and then treated with trifluoroacetic anhydride to give the corresponding *N*-alkyl-3-(trifluoroacetyl)indole (34–36) in a one-pot process. Alkaline hydrolysis induced fluorocarbonyl

elimination²⁹ and furnished, upon workup and recrystallization, the corresponding *N*-alkylindole-3-carboxylic acids (37–39) of analytical purity. Coupling of 37–39 with 19 or 20 using EDC-HOBt yielded 13–18. Indole SCs derived from *L*-valinamide (13, 15, 17) were recrystallized from isopropanol to analytical purity, whereas those comprising *L*-*tert*-leucinamide (14, 16, 18) were purified by flash chromatography owing to their superior solubility in a range of alcoholic solvents.

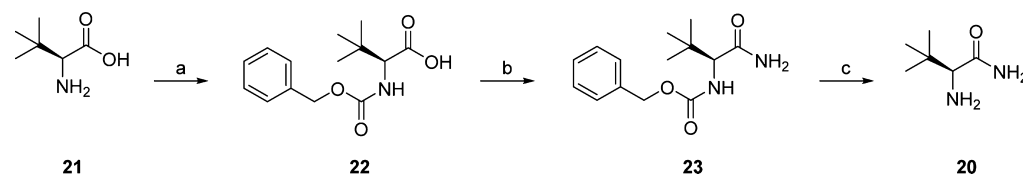
The activity of synthesized indazole (7–12) and corresponding indole (13–18) SCs at CB₁ and CB₂ receptors was evaluated using a fluorometric imaging plate reader (FLIPR) assay to provide structure–activity relationship (SAR) data regarding the choice of heteroaromatic core, amino acid side-chain, and alkyl substituent within this class of SCs. Additionally, the *in vivo* activity of 7 and 9 was compared using biotelemetry in rats to provide information regarding the increasingly common 4-fluorobenzyl motif in SCs.

The cannabimimetic activities of 7–18 were compared to those of phytocannabinoid Δ^9 -THC (a partial agonist at CB₁ and CB₂) and indole SC JWH-018 (a full agonist at CB₁ and CB₂), and the data is presented in Table 1. Murine AtT-20 neuroblastoma cells were stably transfected with human CB₁ or CB₂ receptors, and activities of Δ^9 -THC, JWH-018, and 7–18 were evaluated using a FLIPR membrane potential assay whereby endogenously expressed G protein-gated inwardly rectifying K⁺ channels (GIRKs) are activated by agonists at the expressed CB₁ or CB₂ receptors. The maximum effects of Δ^9 -THC, JWH-018, and 7–18 were compared to high efficacy CB₁/CB₂ receptor agonist CP 55,490, which produced a maximal decrease in fluorescence, corresponding to cellular hyperpolarization, at a concentration of 1 μ M in AtT-20-CB₁ and AtT-20-CB₂ cells. None of the compounds produced a significant change in the membrane potential of wild-type AtT-20 cells, which do not express CB₁ or CB₂ receptors.

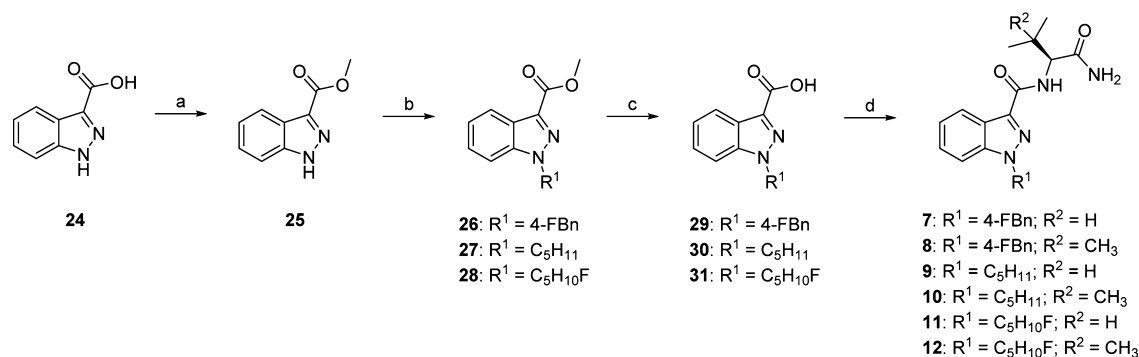
All indole and indazole SCs activated CB₁ and CB₂ receptors. All compounds had greater potency (0.24–21 nM) than Δ^9 -THC (172 nM) for CB₁ receptor-mediated activation of GIRK. Δ^9 -THC is a low-efficacy CB₂ agonist, and in the assay of GIRK activation in AtT-20-CB₂, its effects at 30 μ M were only 32 \pm 1% of that mediated by CP 55,940. CP 55,940 was more potent at stimulating a cellular hyperpolarization in AtT-20-CB₂ cells than AtT-20-CB₁ cells, displaying an approximately 2-fold CB₂ preference. All indazole and indole SCs had a similar maximal effect to CP 55,940 at CB₁ and CB₂ receptors, suggesting that these SCs are also high efficacy agonists. With the exception of 13, all novel SCs showed a mild preference for CB₁ receptors, and it is activation of CB₁ receptors that is associated with the psychoactive effects of cannabinoids.²

The least potent compound in the series (indole 13) was 11-fold more potent than Δ^9 -THC at CB₁ receptors, and the most potent compound (indazole 12) showed more than 1000 times

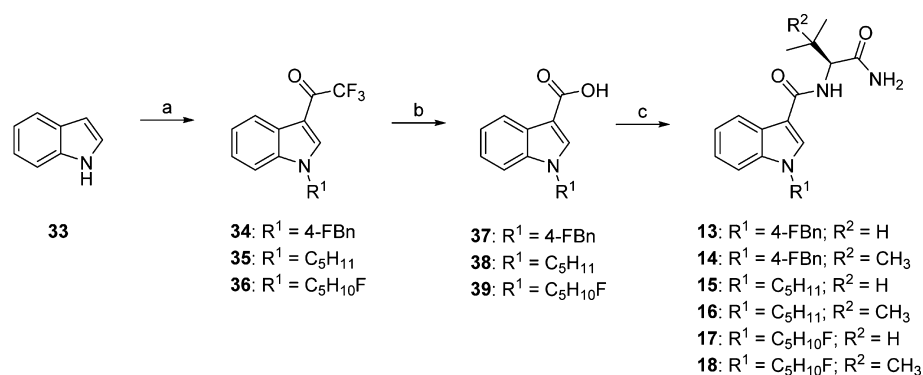
Scheme 1. Synthesis of *L*-*tert*-Leucinamide^a



^aReagents and conditions: (a) NaOH, BnOC(O)Cl, 0 °C to rt, 2 h, 99%; (b) NH₄Cl, Et₃N, HOBt, EDCI, DMF, rt, 16 h, 84%; (c) 10% Pd/C, THF, 48%.

Scheme 2. Synthesis of Indazole SCs 7–12^a

^aReagents and conditions: (a) conc. H₂SO₄, MeOH, reflux, 4 h, 76%; (b) BrR¹, *t*-BuOK, THF, 0 °C to rt, 48 h, 67–77%; (c) NaOH, MeOH, rt, 24 h, 76–96%; (d) EDC·HCl, HOBT, DIPEA, **19** or **20**, DMF, rt, 24 h, 31–63%.

Scheme 3. Synthesis of Indole SCs 13–18^a

^aReagents and conditions: (a) (i) NaH, BrR¹, DMF, 0 °C to rt, 1 h, (ii) (CF₃CO)₂O, DMF, 0 °C to rt, 1 h; (b) KOH, MeOH, PhMe, reflux, 2 h, 54–68% (over two steps); (d) EDC·HCl, HOBT, DIPEA, **19** or **20**, DMF, rt, 24 h, 65–86%.

Table 1. Functional Activity of Δ⁹-THC, CP 55,940, JWH-018, and Novel SCs 7–18 at CB₁ and CB₂ Receptors

compound	hCB ₁		hCB ₂		CB ₁ sel. ^a
	pEC ₅₀ ± SEM (EC ₅₀ , nM)	nax ± SEM (% CP 55,940)	pEC ₅₀ ± SEM (EC ₅₀ , nM)	nax ± SEM (% CP 55,940)	
Δ ⁹ -THC (1)	6.76 ± 0.09 (172)	58 ± 3		32 ± 1 at 30 μM	
CP 55,940 (3)	7.63 ± 0.09 (24)		7.88 ± 0.08 (13)		0.5
JWH-018 (4)	7.74 ± 0.16 (18)	116 ± 9	7.66 ± 0.16 (22)	87 ± 7	1.2
AB-FUBINACA (7)	8.76 ± 0.10 (1.8)	108 ± 7	8.50 ± 0.20 (3.2)	95 ± 12	1.8
ADB-FUBINACA (8)	8.92 ± 0.16 (1.2)	152 ± 11	8.46 ± 0.13 (3.5)	104 ± 7	2.9
AB-PINACA (9)	8.91 ± 0.09 (1.2)	103 ± 4	8.60 ± 0.16 (2.5)	104 ± 8	2.1
ADB-PINACA (10)	9.28 ± 0.08 (0.52)	117 ± 6	9.06 ± 0.31 (0.88)	107 ± 16	1.7
SF-AB-PINACA (11)	9.32 ± 0.10 (0.48)	94 ± 6	8.59 ± 0.25 (2.6)	110 ± 13	5.4
SF-ADB-PINACA (12)	9.61 ± 0.19 (0.24)	91 ± 7	8.68 ± 0.11 (2.1)	94 ± 5	8.8
AB-FUBICA (13)	7.67 ± 0.14 (21)	115 ± 7	7.84 ± 0.27 (15)	99 ± 10	0.7
ADB-FUBICA (14)	8.58 ± 0.15 (2.6)	113 ± 8	8.52 ± 0.16 (3.0)	96 ± 7	1.2
AB-PICA (15)	7.92 ± 0.07 (12)	99 ± 3	7.92 ± 0.21 (12)	94 ± 9	1.0
ADBICA (16)	9.16 ± 0.16 (0.69)	98 ± 7	8.75 ± 0.18 (1.8)	94 ± 7	2.6
SF-AB-PICA (17)	8.28 ± 0.21 (5.2)	123 ± 13	8.05 ± 0.53 (8.9)	121 ± 24	1.7
SF-ADBICA (18)	9.12 ± 0.14 (0.77)	110 ± 7	8.91 ± 0.14 (1.2)	92 ± 6	1.6

^aCB₁ selectivity expressed as the ratio of CB₁ EC₅₀ to CB₂ EC₅₀.

the potency of Δ⁹-THC, making SF-ADB-PINACA one of the most potent SC designer drugs reported to date. Excluding **7** and **8**, indazoles and indoles containing the *L*-*tert*-leucinamide group were more potent at both CB₁ and CB₂ receptors than the corresponding SC featuring an *L*-valinamide substituent. In the most dramatic example, the additional methyl group of **16** (EC₅₀ = 0.68 nM) conferred a 17-fold increase in potency over

15 (EC₅₀ = 12 nM) at CB₁ receptors. The same trend was observed for CB₂ receptors, but potency enhancement was more moderate, with **18** (EC₅₀ = 1.2 nM) showing a 7-fold improvement over **17** (EC₅₀ = 1.2 nM).

Surprisingly, there were no clear trends for differences of potency or efficacy between indazole SCs **7–12** and the corresponding indoles **13–18**. Similarly, choice of *N*-alkyl

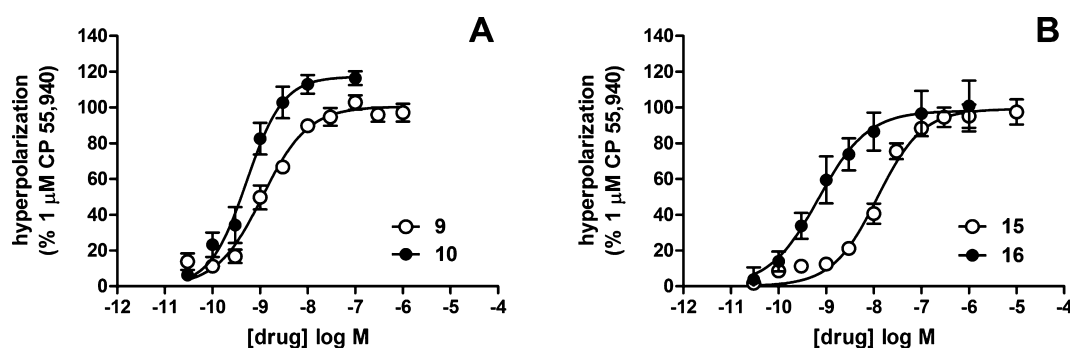


Figure 4. Hyperpolarization of CB₁ receptors induced by (A) AB-PINACA (9) and ADB-PINACA (10) and (B) AB-PICA (15) and ADBICA (16) as a proportion of that produced by 1 μ M CP 55,940. Membrane potential was measured using a fluorescent dye, as outlined in the Methods. Each point represents the mean \pm SEM of at least five independent determinations, each performed in duplicate. Data was fitted with a four-parameter logistic equation in GraphPad Prism.

group had little effect on potency. However, indoles containing the *L*-valinamide group (13, 15, 17), the least potent SCs identified in this series, were each less potent than the corresponding indazoles (7, 9, 11). Taken together, these results suggest that the heteroaromatic core and indole nitrogen substituent of these SCs contribute less to the activity of these compounds than the pendant amide group. The difference in CB₁ activity between *L*-valinamide and *L*-*tert*-leucinamide derivatives featuring a 1-pentyl group and containing an indazole core (9 and 10, respectively) or an indole core (15 and 16, respectively) is depicted in Figure 4.

Very little is known about the potency and psychoactivity of newer SCs in humans. Having demonstrated that 7–18 are potent and efficacious cannabimimetic agents *in vitro*, we sought to demonstrate activity of some of these SCs *in vivo*. Cross-substitution of older SCs, like JWH-018, with Δ^9 -THC has been demonstrated.^{30–32} Cannabinoids are known to induce hypothermia and bradycardia in rats, effects that are common to phytocannabinoids like Δ^9 -THC and heteroaromatic SCs such as JWH-018.^{33–35} We have previously evaluated the hypothermic and bradycardic potencies of Δ^9 -THC and numerous structurally diverse SCs including JWH-018, AM-2201, UR-144, XLR-11, PB-22, 5F-PB-22, APICA, and STS-135.^{14,36} The cannabimimetic activities AB-FUBINACA and AB-PINACA were evaluated using radiotelemetry in male Wistar rats, and the effects of these SCs on body temperature (Figure 5) and heart rate (Figure 6) are presented below.

Rat body temperature 1 h prior to intraperitoneal (i.p.) injection and 6 h postinjection of AB-FUBINACA and AB-PINACA are presented in 15 min bins in Figure 5. For each drug, these data are presented for 1 h before (baseline) and 6 h after injection of various doses. The dashed line on the figures represents the time of SC injection. Each SC was investigated using a cohort of 3–4 rats, with a different cohort used for the two compounds. Doses were escalated from 0 mg/kg (baseline) to 0.1, 0.3, 1, and 3 mg/kg for each compound, with at least two washout days between each dose. The 0.1 mg/kg doses of each compound were without significant effects on body temperature and heart rate, so data for these doses are not presented.

A substantial hypothermic effect was evoked by 0.3–3 mg/kg of both drugs, with the peak reduction in body temperature generally greater with AB-FUBINACA (>2 °C) than AB-PINACA (>1.5 °C). As Figure 5 shows, the 4-fluorobenzyl-substituted AB-FUBINACA appeared to confer a hypothermic

effect of greater magnitude and duration (~4 h) than that observed for the pentyl-substituted AB-PINACA (~2 h) at the same dose (3 mg/kg). This was verified by a statistical analysis showing a significantly greater area under the curve for body temperature (relative to vehicle baseline) for AB-FUBINACA doses compared to that for AB-PINACA at 3 mg/kg ($P < 0.05$).

Results for heart rate are presented in 30 min bins in Figure 6, with the dashed line on the figures again representing the time of SC injection. Results were consistent with body temperature data, although data were generally more variable than they were with body temperature data, reflecting the multiple determinants of heart rate including locomotor activity, stress, and direct cardiovascular pharmacological effects. All doses shown produced a significant decrease in heart rate, with statistically significant treatment or treatment by time effects at these doses (ANOVA, planned contrasts, SC dose versus vehicle, $P < 0.05$).

To confirm that the observed effects were mediated through CB₁ or CB₂ receptors, the reversibility of the effects of AB-PINACA and AB-FUBINACA on body temperature and heart rate in rats following pretreatment with either CB₁ receptor antagonist rimonabant (SR141176, 40, Figure 7) or CB₂ receptor antagonist SR144528 (41) was assessed. Rimonabant is a potent, selective, CB₁ receptor neutral antagonist that reverses CB₁-mediated cannabinoid agonist effects in rodents and humans,^{2,37,38} whereas SR144528 is selective CB₂ antagonist/inverse agonist.^{39,40}

Rat body temperatures after injection (i.p.) with vehicle, CB₁ antagonist (rimonabant, 3 mg/kg), or CB₂ antagonist (SR144528, 3 mg/kg) 30 min prior to treatment with either AB-FUBINACA (3 mg/kg) or AB-PINACA (3 mg/kg) are presented in 15 min bins in Figure 8. For each treatment condition, these data are presented for 1 h before (baseline) and 6 h after injection of various doses. The first dashed line on the figure represents the time of vehicle/antagonist injection, and the second dashed line represents time of SC injection. Each SC was investigated using a cohort of 3–4 rats, with a different cohort used for the two compounds. The dose of each antagonist was 3 mg/kg, and the dose of each SC was also 3 mg/kg.

Pretreatment with rimonabant was able to completely reverse the hypothermic effects of AB-FUBINACA, whereas pretreatment with SR144528 had no effect on the body temperature decrease induced by AB-FUBINACA (Figure 8A). Similarly, rimonabant partially reversed the decreased body temperature effected by AB-PINACA, but SR144528 had negligible effect on

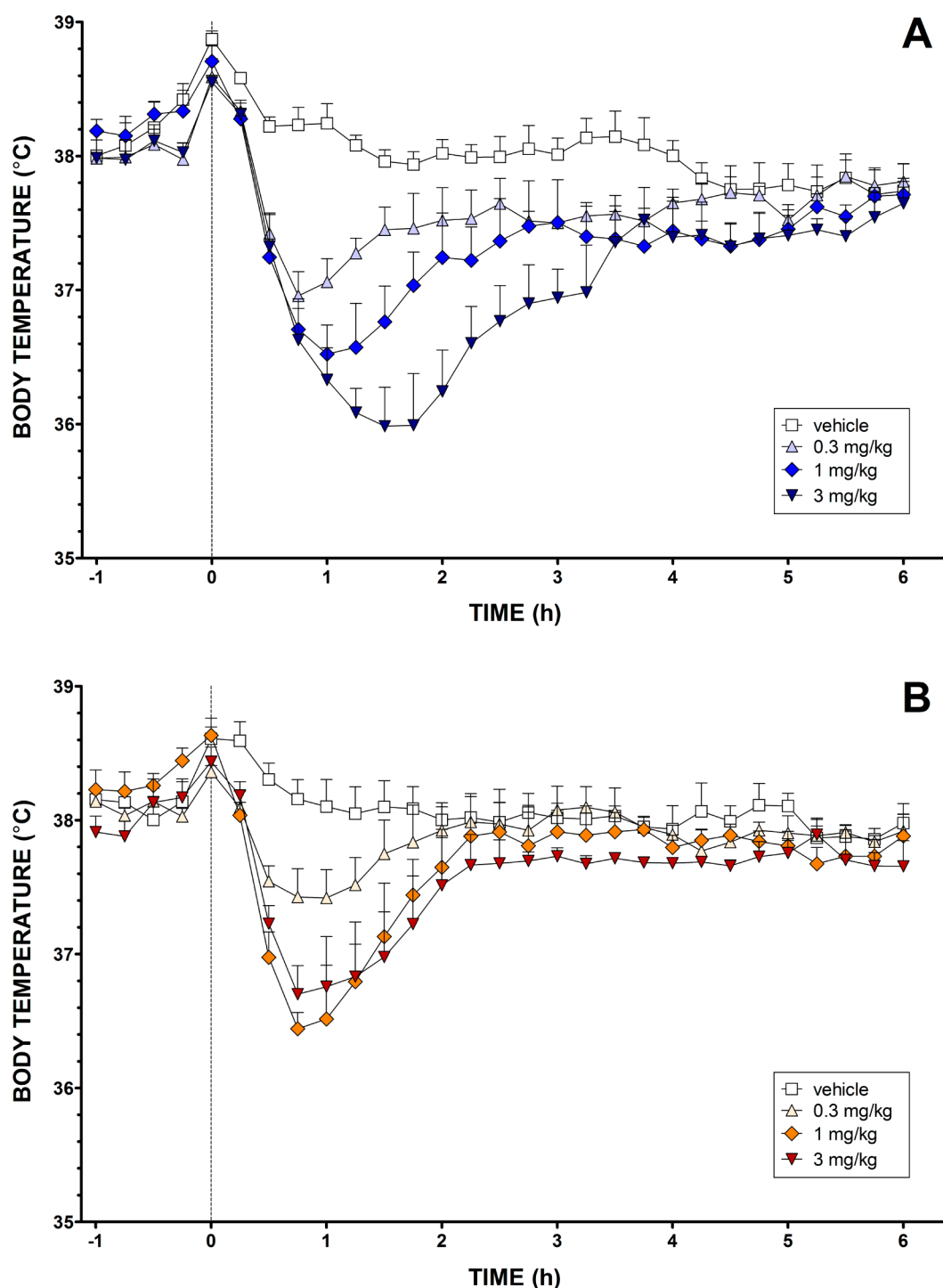


Figure 5. Effects of (A) AB-FUBINACA and (B) AB-PINACA on rat body temperature. Dashed line denotes time of intraperitoneal injection. Each point represents the mean \pm SEM for three animals.

AB-PINACA-induced hypothermia (Figure 8B). These interpretations are confirmed by a statistical analysis of the areas between each drug treatment and baseline (Figure S13, Supporting Information). This suggests a CB_1 -mediated hypothermic mechanism. Similar trends were observed for the reversal of AB-FUBINACA- or AB-PINACA-induced bradycardia by rimonabant but not SR144528; however, these differences did not reach significance (data not shown). This is likely due to a combination of the relatively smaller magnitude

of SC-induced bradycardic effects and high variability of the heart rate data.

CONCLUSIONS

This study is the first to pharmacologically characterize the emergent class of recreational SC designer drugs based on indole and indazole scaffolds and featuring *L*-valinamide or *L*-*tert*-leucinamide side chains. Synthetic routes to identified SCs of forensic interest (AB-FUBINACA, ADB-FUBINACA, AB-PINACA, ADB-PINACA, 5F-AB-PINACA, 5F-ADB-PINACA,

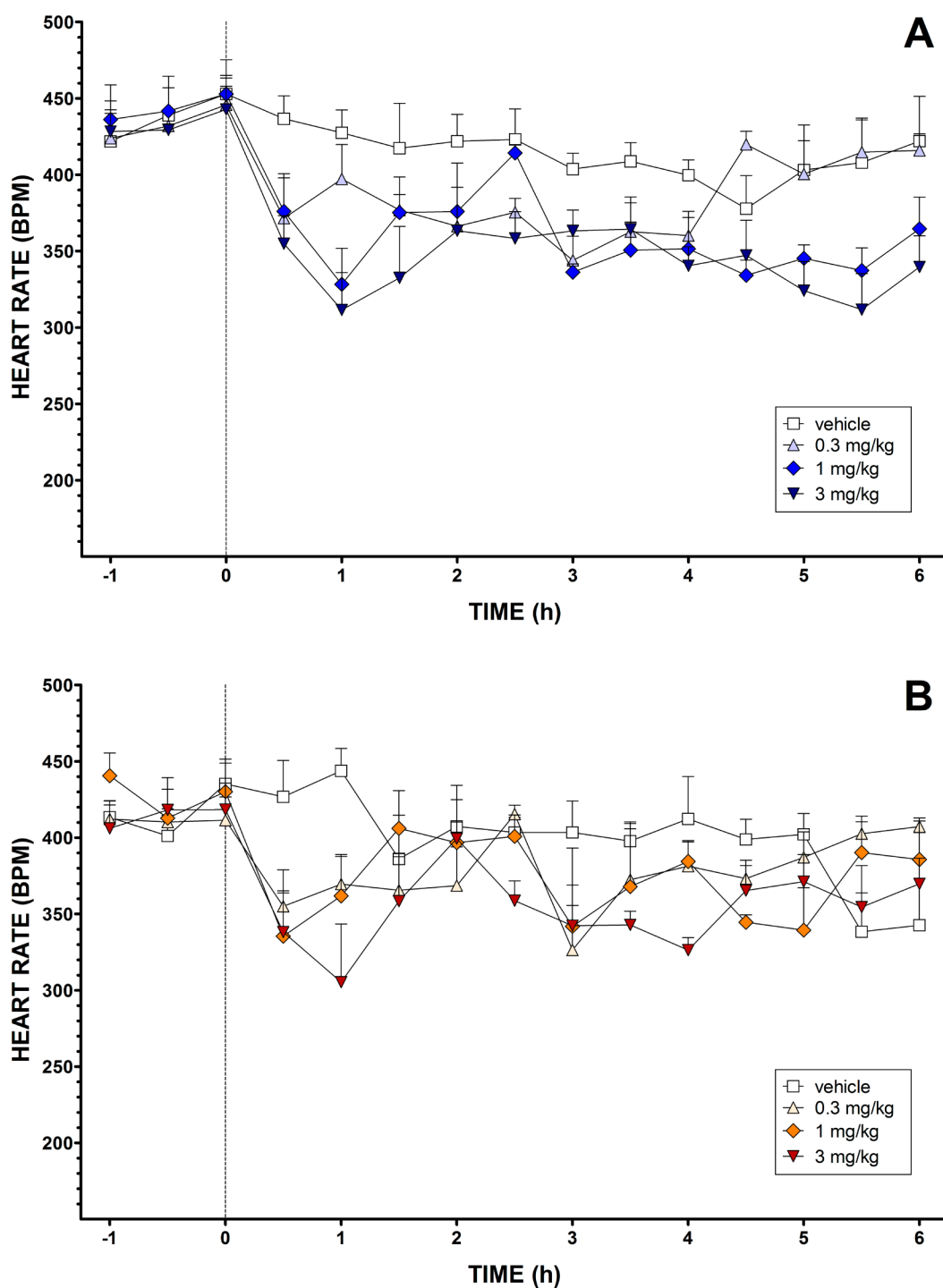


Figure 6. Effects of (A) AB-FUBINACA and (B) AB-PINACA on rat heart rate. Dashed line denotes time of intraperitoneal injection. Each point represents the mean \pm SEM for three animals.

ADBICA, 5F-ADBICA), as well as several undetected analogues, were developed. These synthetic routes are general for 1-alkyl-1*H*-indazole-3-carboxamides and 1-alkyl-1*H*-indole-3-carboxamides and enable forensic chemists to proactively develop reference standards for structurally related SCs expected to appear in the future. All synthesized SCs acted as agonists of CB₁ and CB₂ receptors in a FLIPR membrane potential assay and thus are functional cannabinoids. Preliminary SARs suggest that *L*-tert-leucinamide derivatives possess greater potency at CB₁ receptors *in vitro* than the corresponding *L*-valinamide analogues. The most potent of

these was 5F-ADB-PINACA. In rats, AB-FUBINACA and AB-PINACA were able to dose-dependently decrease body temperature and heart rate at doses of 0.3–3 mg/kg, indicating that these SCs are also cannabimimetic *in vivo*. AB-FUBINACA had more potent effects on body temperature than AB-PINACA. The hypothermic effects of AB-FUBINACA and AB-PINACA appear to be mediated through CB₁ receptors and could be reversed by pretreatment with CB₁ antagonist rimonabant but not CB₂ antagonist SR144528. Both *in vitro* and *in vivo* results confirm that all of the SCs explored have

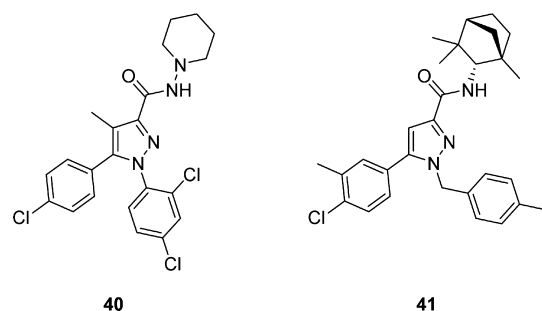


Figure 7. Structures of selective CB₁ receptor antagonist rimonabant (SR141176, **40**) and selective CB₂ receptor antagonist SR144528 (**41**).

cannabinimetic effects that parallel those of Δ^9 -THC, but with greater potency.

METHODS

General Chemical Synthesis Details. All reactions were performed under an atmosphere of nitrogen unless otherwise specified. Commercially available chemicals were used as purchased. Flash column chromatography was performed using Merck Kieselgel 60 (230–400 mesh) silica gel. Melting points were measured in open capillaries using a Gallenkamp 5A 6797 melting point apparatus and are uncorrected. Nuclear magnetic resonance spectra were recorded at 300 K using a Bruker 300, 400, or 500 MHz spectrometer. The data are reported as chemical shift (δ ppm) relative to the residual protonated solvent resonance, relative integral, multiplicity (s = singlet, bs = broad singlet, d = doublet, t = triplet, q = quartet, quin. = quintet, m = multiplet, dd = doublet of doublets, dt = doublet of triplets, qd = quartet of doublets), coupling constants (J Hz), and assignment. Low-resolution mass spectra (LRMS) were recorded using electrospray ionization (ESI) recorded on a Finnigan LCQ ion trap spectrometer. HPLC analysis of the organic purity of the compounds submitted for *in vivo* testing (4–7) was conducted on a Waters e2695 separations module using a Waters Sunfire C18 5 μ m, 2.1 \times 150 mm column and detected using a Waters 2489 UV/vis detector set at 254 nm. Separation was achieved using water with 0.1% formic acid (solvent A) and acetonitrile with 0.1% formic acid (solvent B) at a flow rate of 0.2 mL/min and a gradient of 5% B for 1 min, then 5–100% B over 30 min. Elemental analysis was obtained from the Chemical Analysis Facility in the Department of Chemistry and Biomolecular Sciences, Macquarie University, Australia.

General Procedure A: Amidation of 1-Alkyl-1H-indazole-3-carboxylic Acids and 1-Alkylindole-3-carboxylic Acids. A solution of the appropriate carboxylic acid **29**, **30**, **31**, **37**, **38**, or **39** (7.5 mmol, 1.5 equiv) in DMF (50 mL) was treated with EDC (7.5 mmol, 1.5 equiv), HOBT (7.5 mmol, 1.5 equiv), DIPEA (25.5 mmol, 5.1 equiv), **19**·HCl, or **20** (5 mmol) and stirred for 24 h. The mixture was partitioned between and H₂O (100 mL) and EtOAc (50 mL), the layers were separated, and the aqueous layer was extracted with EtOAc (2 \times 50 mL). The combined organic phases were dried (MgSO₄), and the solvent was evaporated under reduced pressure. The crude products were purified by flash chromatography and/or recrystallization.

(*S*)-*N*-(1-Amino-3-methyl-1-oxobutan-2-yl)-1-(4-fluorobenzyl)-1H-indazole-3-carboxamide (AB-FUBINACA, **7**). Treating **29** (1.20 g, 4.4 mmol) with **19** (1.04 g, 6.8 mmol) according to general procedure A gave, following purification by flash chromatography (hexane–EtOAc, 10:90), **7** (0.94 g, 57%) as a white solid. Recrystallization from *i*-PrOH–H₂O yielded material of analytical purity. mp 151–152 °C; ¹H NMR (500 MHz, CDCl₃): δ 8.33 (1H, d), 7.54 (1H, d, J = 8.9 Hz), 7.37 (1H, m), 7.32 (1H, m), 7.27 (1H, m), 6.39 (1H, bs), 5.69 (1H, bs), 5.57 (2H, s), 4.58 (1H, dd, J = 8.9 Hz, 6.8 Hz), 2.35 (1H, dq, J = 13.6 Hz, 6.8 Hz), 1.09 (6H, dd, J = 7.2 Hz, 5.1 Hz); ¹³C NMR (125 MHz, CDCl₃): δ 173.7 (CO), 162.9 (CO), 162.6 (d, ¹*J*_{C–F} = 249.1 Hz, quat.), 140.9 (quat.), 137.3 (quat.), 131.7 (d, ⁴*J*_{C–F} = 3.4 Hz,

quat.), 129.2 (d, ³*J*_{C–F} = 8.3 Hz, CH), 127.3 (CH), 123.4 (quat.), 123.1 (CH), 122.8 (CH), 116.0 (d, ²*J*_{C–F} = 21.6 Hz, CH), 109.7 (CH), 58.0 (CH), 53.1 (CH₂), 30.8 (CH), 19.6 (CH₃), 18.4 (CH₃); ¹⁹F NMR (470 MHz, CDCl₃): δ –113.9 ppm; LRMS (+ESI): *m/z* 323.9 ([M – CONH₃]⁺, 100%), 351.8 ([M – NH₃]⁺, 50%), 368.8 ([M + H]⁺, 20%); Anal. Calcd for C₂₀H₂₁N₄O₂F: C, 65.20; H, 5.75; N, 15.21. Found: C, 65.28; H, 5.73; N, 15.21; HPLC purity: 99.2%.

(*S*)-*N*-(1-Amino-3,3-dimethyl-1-oxobutan-2-yl)-1-(4-fluorobenzyl)-1H-indazole-3-carboxamide (ADB-FUBINACA, **8**). Treating **29** (0.51 g, 1.9 mmol) with **20** (0.37 g, 2.8 mmol) according to general procedure A gave, following purification by flash chromatography (hexane–EtOAc, 10:90), **8** (0.22 g, 31%) as a white solid. mp 135–137 °C; NMR (500 MHz, CDCl₃): δ 8.21 (1H, d, J = 8.0 Hz), 7.72 (1H, d, J = 9.7 Hz), 7.27 (1H, m), 7.19 (1H, m), 7.14 (2H, dd, J = 8.3 Hz, 5.4 Hz), 6.99 (1H, bs), 6.93 (2H, t, J = 8.6 Hz), 6.16 (1H, bs), 5.52 (2H, s), 4.74 (1H, d, 9.6 Hz), 1.15 (1H, s), 1.11 (9H, s); ¹³C NMR (125 MHz, CDCl₃): δ 173.5 (CO), 162.6 (CO), 162.6 (d, ¹*J*_{C–F} = 245.8 Hz, quat.), 140.9 (quat.), 137.3 (quat.), 131.8 (d, ⁴*J*_{C–F} = 3.1 Hz, quat.), 129.1 (d, ³*J*_{C–F} = 8.3 Hz, CH), 127.1 (CH), 123.4 (quat.), 123.0 (CH), 122.6 (CH), 115.9 (d, ²*J*_{C–F} = 21.6 Hz, CH), 109.7 (CH), 59.7 (CH), 53.1 (CH₂), 34.8 (quat.), 26.9 (CH₃); ¹⁹F NMR (470 MHz, CDCl₃): δ –113.9; LRMS (+ESI): *m/z* 337.9 ([M – CONH₃]⁺, 100%), 365.8 ([M – NH₃]⁺, 50%), 382.7 ([M + H]⁺, 21%); Anal. Calcd for C₂₁H₂₃N₄O₂F: C, 65.95; H, 6.06; N, 14.65. Found: C, 65.38; H, 6.08; N, 14.38.

(*S*)-*N*-(1-Amino-3-methyl-1-oxobutan-2-yl)-1-pentyl-1H-indazole-3-carboxamide (AB-PINACA, **9**). Treating **30** (0.50 g, 2.2 mmol) with **19** (0.50 g, 3.3 mmol) according to general procedure A gave, following purification by flash chromatography (hexane–EtOAc, 50:50), **9** (0.44 g, 62%) as a white solid. Recrystallization from EtOAc–hexane yielded material of analytical purity. mp 125–126 °C; ¹H NMR (500 MHz, CDCl₃): δ 8.30 (1H, d, J = 8.3 Hz), 7.51 (1H, d, J = 8.8 Hz), 7.45–7.37 (2H, m), 7.26 (1H, m), 6.51 (1H, bs), 5.75 (1H, bs), 4.86 (1H, m), 4.38 (2H, t, J = 7.2 Hz), 2.36 (1H, dq, J = 13.6 Hz, 6.9 Hz), 1.94 (2H, quin., J = 7.4 Hz), 1.43–1.25 (4H, m), 1.08 (6H, m), 0.89 (3H, t, J = 7.1 Hz); ¹³C NMR (125 MHz, CDCl₃): δ 173.9 (CO), 163.2 (CO), 141.0 (quat.), 136.5 (quat.), 126.8 (CH), 123.0 (quat.), 122.8 (CH), 122.7 (CH), 109.5 (CH), 57.9 (CH), 49.7 (CH₂), 30.7 (CH), 29.5 (CH₂), 29.1 (CH₂), 22.4 (CH₂), 19.6 (CH₃), 18.3 (CH₃), 14.0 (CH₃); LRMS (+ESI): *m/z* 258.9 ([M – CONH₃]⁺, 100%), 313.9 ([M – NH₃]⁺, 88%), 330.8 ([M + H]⁺, 46%); Anal. Calcd for C₁₈H₂₆N₄O₂: C, 65.43; H, 7.93; N, 16.96. Found: C, 65.75; H, 8.11; N, 16.98; HPLC purity: 97.6%.

(*S*)-*N*-(1-Amino-3,3-dimethyl-1-oxobutan-2-yl)-1-pentyl-1H-indazole-3-carboxamide (ADB-PINACA, **10**). Treating **30** (0.50 g, 2.2 mmol) with **20** (0.43 g, 3.3 mmol) according to general procedure A gave, following purification by flash chromatography (hexane–EtOAc, 50:50), **10** (0.46 g, 63%) as a white solid. mp 135–137 °C; NMR (400 MHz, CDCl₃): δ 8.27 (1H, m), 7.71 (1H, d, J = 9.5 Hz), 7.45–7.36 (2H, m), 7.29–7.22 (1H, m), 6.65 (1H, bs), 5.80 (1H, bs), 4.69 (1H, d, J = 9.5 Hz), 4.38 (2H, t, J = 7.2 Hz), 1.95 (2H, quin., J = 7.2 Hz), 1.45–1.25 (4H, m), 1.16 (9H, s), 0.89 (3H, t, J = 7.0 Hz); ¹³C NMR (100 MHz, CDCl₃): δ 173.2 (CO), 162.8 (CO), 141.0 (quat.), 136.5 (quat.), 126.7 (CH), 123.0 (quat.), 122.7 (CH), 122.5 (CH), 109.5 (CH), 59.7 (CH), 49.6 (CH₂), 34.8 (quat.), 29.5 (CH₂), 29.0 (CH₂), 26.9 (CH₃), 22.3 (CH₂), 14.0 (CH₃); LRMS (+ESI): *m/z* 299.9 ([M – CONH₃]⁺, 100%), 327.9 ([M – NH₃]⁺, 59%), 344.8 ([M + H]⁺, 19%); Anal. Calcd for C₁₉H₂₈N₄O₂: C, 66.25; H, 8.19; N, 16.27. Found: C, 66.45; H, 8.40; N, 16.29.

(*S*)-*N*-(1-Amino-3-methyl-1-oxobutan-2-yl)-1-(5-fluoropentyl)-1H-indazole-3-carboxamide (5F-AB-PINACA, **11**). Treating **31** (1.10 g, 4.4 mmol) with **19** (1.00 g, 6.7 mmol) according to general procedure A gave, following purification by flash chromatography (hexane–EtOAc, 10:90), **11** (0.56 g, 37%). Recrystallization from EtOAc–hexane yielded material of analytical purity. mp 110–111 °C; ¹H NMR (500 MHz, CDCl₃): δ 8.30 (1H, m), 7.51 (1H, d, J = 8.9 Hz), 7.45–7.39 (2H, m), 7.27 (1H, m), 6.48 (1H, bs), 5.74 (1H, bs), 4.58 (1H, dd, J = 9.1 Hz, 6.7 Hz), 4.47 (1H, t, J = 6.0 Hz), 4.43–4.36 (3H, m), 2.35 (1H, dq, J = 13.6 Hz, 6.8 Hz), 2.00 (2H, m), 1.80–1.66 (2H, m), 1.51–1.41 (2H, m), 1.08 (6H, dd, J = 7.1 Hz, 5.2 Hz); ¹³C

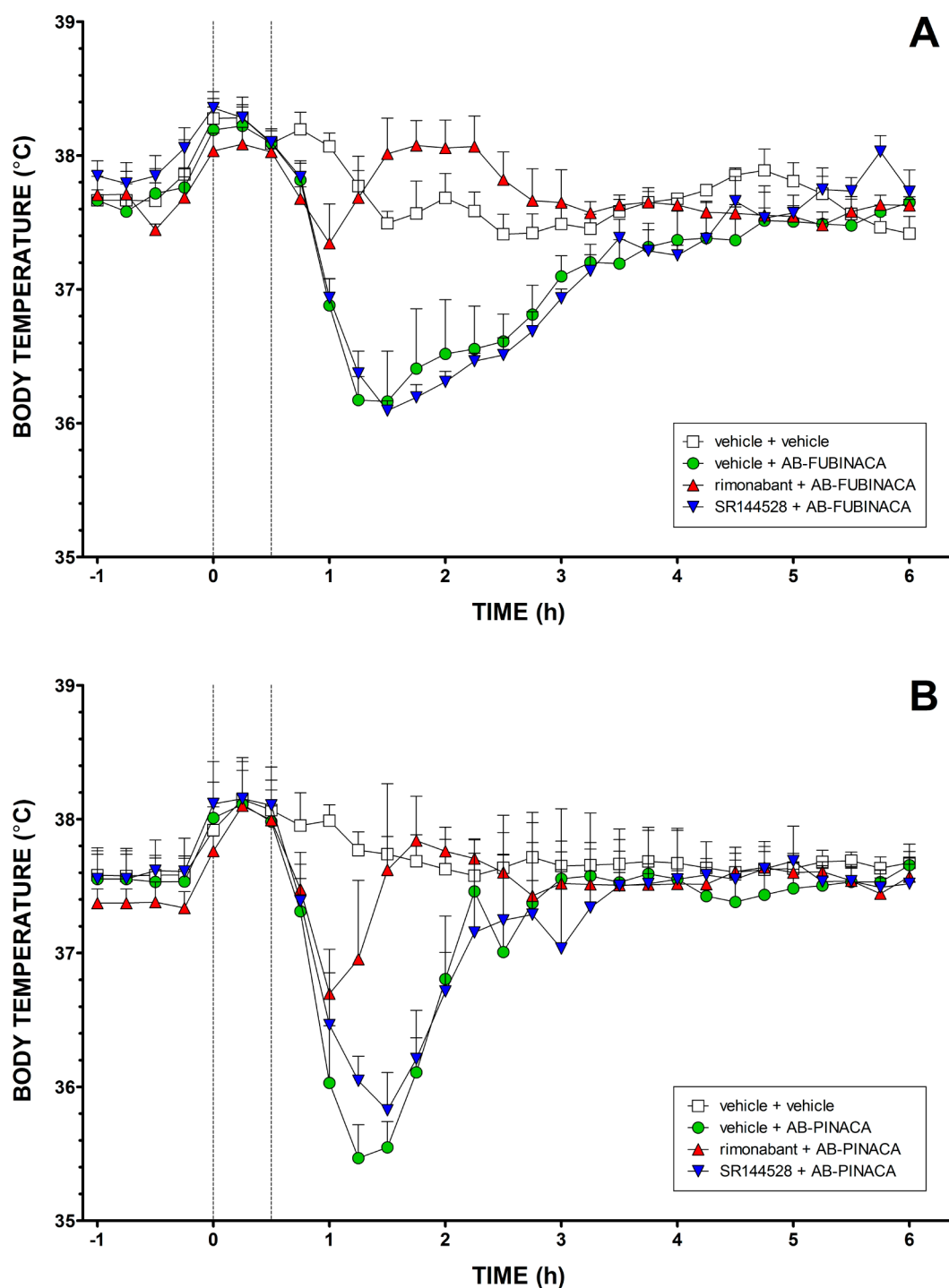


Figure 8. Effects of 3 mg/kg of (A) AB-FUBINACA or (B) AB-PINACA on rat body temperature following pretreatment (30 min prior) with vehicle, 3 mg/kg rimonabant (CB_1 antagonist), or 3 mg/kg SR144528 (CB_2 antagonist). The first dashed line denotes time of intraperitoneal injection of vehicle or antagonist. Second dashed line represents time of intraperitoneal injection of SC. Each point represents the mean \pm SEM for three animals.

NMR (125 MHz, $CDCl_3$): δ 173.8 (CO), 163.0 (CO), 141.0 (quat.), 136.6 (quat.), 126.9 (CH), 122.99 (quat.), 122.91 (CH), 122.7 (CH), 109.4 (CH), 83.8 (CH_2 , d, $^1J_{C-F}$ = 164.0 Hz), 57.9 (CH), 49.3 (CH_2), 30.7 (CH), 30.0 (CH_2 , d, $^2J_{C-F}$ = 20.1 Hz), 29.4 (CH_2), 22.8 (CH_2 , d, $^3J_{C-F}$ = 5.1 Hz), 19.6 (CH_3), 18.3 (CH_3); ^{19}F NMR (470 MHz, $CDCl_3$): δ -218.6; LRMS (ESI): m/z 303.9 ($[M - CONH_3]^+$, 100%), 331.9 ($[M - NH_3]^+$, 59%), 348.9 ($[M + H]^+$, 48%); Anal. Calcd for $C_{18}H_{25}N_4O_2F$: C, 62.05; H, 7.23; N, 16.08. Found: C, 61.96; H, 7.26; N, 15.83.

(*S*)-*N*-(1-Amino-3,3-dimethyl-1-oxobutan-2-yl)-1-(5-fluoropentyl)-1*H*-indazole-3-carboxamide (5*F*-AD*B*-PINACA, **12**). Treating **31** (0.40 g, 1.6 mmol) with **20** (0.32 g, 2.4 mmol) according to general procedure A gave, following purification by flash chromatography (hexane–EtOAc, 10:90), **12** (0.27 g, 47%) as a white solid. mp 135–137 °C; 1H NMR (400 MHz, $CDCl_3$): δ 8.28 (1H, d, J = 8.2 Hz), 7.70 (1H, 9.4 Hz), 7.45–7.38 (2H, m), 7.30–7.23 (1H, m), 6.53 (1H, bs), 5.75 (1H, bs), 4.66 (1H, d, J = 9.6 Hz), 4.45–4.33 (3H, m), 2.18 (1H, bs), 2.00 (2H, quin., J = 7.7 Hz), 1.84–1.64 (2H, m), 1.48 (2H, m), 1.16 (9H, s); ^{13}C NMR (100 MHz, $CDCl_3$): δ 173.1 (CO), 162.8

(CO), 141.0 (quat.), 136.8 (quat.), 126.9 (CH), 123.0 (quat.), 122.8 (CH), 122.7 (CH), 109.4 (CH), 83.9 (d, $^1J_{C-F}$ = 164.6, CH₂), 59.8 (CH), 49.4 (CH₂), 34.8 (quat.), 30.0 (d, $^2J_{C-F}$ = 19.7 Hz, CH₂), 29.4 (CH₂), 26.9 (CH₃), 22.8 (d, $^3J_{C-F}$ = 5.1 Hz, CH₂); ^{19}F NMR (376 MHz, CDCl₃): δ -218.3; LRMS (+ESI): m/z 317.9 ([M - CONH₃]⁺, 100%), 345.9 ([M - NH₃]⁺, 50%), 362.8 ([M + H]⁺, 17%); Anal. Calcd for C₁₉H₂₇N₄O₂F: C, 62.96; H, 7.51; N, 15.46. Found: C, 63.12; H, 7.57; N, 15.29.

(*S*)-*N*-(1-Amino-3-methyl-1-oxobutan-2-yl)-1-(4-fluorobenzyl)-1*H*-indole-3-carboxamide (AB-FUBICA, **13**). Treating **37** (1.20 g, 4.5 mmol) with **19** (1.03 g, 6.7 mmol) according to general procedure A gave, following recrystallization from *i*-PrOH, **13** (1.28 g, 82%) as a white solid. mp 212–214 °C; 1H NMR (300 MHz, DMSO-*d*₆): δ 8.53 (1H, bs), 8.11 (1H, m), 7.64–7.50 (2H, m), 7.48 (1H, bs), 7.41–7.27 (2H, m), 7.24–7.10 (4H, m), 7.07 (1H, bs), 5.45 (2H, m), 4.36 (1H, m), 2.09 (1H, m), 0.94 (6H, dd, J = 6.7 Hz, 2.7 Hz); ^{13}C NMR (75 MHz, DMSO-*d*₆): δ 173.5 (CO), 164.0 (CO), 161.6 (quat., d, $^1J_{C-F}$ = 243.18 Hz), 136.0 (CH), 133.7 (quat., d, $^4J_{C-F}$ = 2.87 Hz), 131.6 (quat.), 129.3 (d, $^3J_{C-F}$ = 8.1 Hz, CH), 126.7 (CH), 122.1 (CH), 121.1 (CH), 120.8 (CH), 115.5 (d, $^2J_{C-F}$ = 21.4 Hz, CH), 110.6 (quat.), 110.0 (CH), 57.4 (CH), 48.7 (CH₂), 30.4 (CH), 19.5 (CH₃), 18.5 (CH₃); ^{19}F NMR (282 MHz, DMSO-*d*₆): δ -114.9 (m); LRMS (+ESI): m/z 350.9 ([M - NH₃]⁺, 100%), 367.8 ([M + H]⁺, 70%); Anal. Calcd for C₂₁H₂₂N₃O₂F: C, 68.65; H, 6.04; N, 11.44. Found: C, 68.88; H, 6.15; N, 11.37; HPLC purity: 99.4%.

(*S*)-*N*-(1-Amino-3,3-dimethyl-1-oxobutan-2-yl)-1-(4-fluorobenzyl)-1*H*-indole-3-carboxamide (ADB-FUBICA, **14**). Treating **37** (0.63 g, 2.3 mmol) with **20** (0.46 g, 3.5 mmol) according to general procedure A gave, following purification by flash chromatography (hexane–EtOAc, 10:90), **14** (0.76 g, 86%) as a white solid. mp 107–108 °C; 1H NMR (400 MHz, CDCl₃): δ 8.03 (1H, d, J = 7.7 Hz), 7.73 (1H, s), 7.31–7.20 (4H, m), 7.14–7.06 (2H, m), 6.99 (2H, t, J = 8.6 Hz), 6.77 (1H, d, J = 9.2 Hz), 6.54 (1H, bs), 5.71 (1H, bs), 5.27 (2H, s), 4.71 (1H, d, J = 9.2 Hz), 1.14 (9H, s); ^{13}C NMR (100 MHz, CDCl₃): δ 173.4 (CO), 165.0 (CO), 162.6 (d, $^1J_{C-F}$ = 247.2 Hz, quat.), 136.8 (CH), 132.0 (d, $^4J_{C-F}$ = 3.2 Hz, quat.), 131.8 (quat.), 128.8 (d, $^3J_{C-F}$ = 8.1 Hz, CH), 125.8 (quat.), 123.1 (CH), 122.1 (CH), 120.5 (CH), 116.6 (d, $^2J_{C-F}$ = 21.6 Hz, CH), 111.4 (quat.), 110.7 (CH), 59.9 (CH), 50.1 (CH₂), 34.9 (quat.), 27.0 (CH₃); ^{19}F NMR (376 MHz, CDCl₃): δ -113.9; LRMS (+ESI): m/z 363.9 ([M - NH₃]⁺, 100%), 381.8 ([M + H]⁺, 42%); Anal. Calcd C₂₂H₂₄N₃O₂F: C, 69.27; H, 6.34; N, 11.02. Found: C, 69.68; H, 6.02; N, 10.95.

(*S*)-*N*-(1-Amino-3-methyl-1-oxobutan-2-yl)-1-pentyl-1*H*-indole-3-carboxamide (AB-PICA, **15**). Treating **38** (0.50 g, 2.2 mmol) with **19** (0.50, 3.3 mmol) according to general procedure A gave, following purification by flash chromatography (hexane–EtOAc, 10:90), **15** (0.58 g, 81%) as a white solid. mp 214–215 °C; 1H NMR (400 MHz, DMSO-*d*₆): δ 8.25 (1H, s), 8.11 (1H, d, J = 7.7 Hz), 7.61–7.39 (3H, m), 7.20 (1H, m), 7.13 (1H, t, J = 7.6 Hz), 7.06 (1H, bs), 4.35 (1H, m), 4.19 (2H, m), 2.09 (1H, dq, J = 13.5 Hz, 6.8 Hz), 1.08 (2H, quin., J = 7.3 Hz), 1.39–1.19 (4H, m), 0.94 (6H, dd, J = 6.6 Hz, 3.1 Hz), 0.85 (3H, t, J = 7.0 Hz); ^{13}C NMR (100 MHz, DMSO-*d*₆): δ 173.6 (CO), 164.0 (CO), 136.1 (CH), 131.2 (quat.), 126.5 (quat.), 121.8 (CH), 121.0 (CH), 120.6 (CH), 110.3 (quat.), 109.3 (CH), 57.3 (CH), 45.8 (CH₂), 30.3 (CH), 29.3 (CH₂), 28.4 (CH₂), 21.7 (CH₂), 19.5 (CH₂), 18.5 (CH₃), 13.8 (CH₃); LRMS (+ESI): m/z 312.87 ([M - NH₃]⁺, 100%), 329.80 ([M + H]⁺, 60%); Anal. Calcd for C₁₉H₂₇N₃O₂: C, 69.27; H, 8.26; N, 12.76. Found: C, 69.21; H, 8.66; N, 12.55; HPLC purity: 99.1%.

(*S*)-*N*-(1-Amino-3,3-dimethyl-1-oxobutan-2-yl)-1-pentyl-1*H*-indole-3-carboxamide (ADBICA, **16**). Treating **38** (0.57 g, 2.5 mmol) with **20** (0.49 g, 3.7 mmol) according to general procedure A gave, following purification by flash chromatography (hexane–EtOAc, 10:90), **16** (0.64 g, 75%) as a white solid. mp 138–139 °C; 1H NMR (400 MHz, CDCl₃): δ 8.01 (1H, m), 7.72 (1H, s), 7.38 (1H, m), 7.33–7.22 (2H, m), 6.74 (1H, d, J = 8.9 Hz), 6.60 (1H, bs), 5.71 (1H, bs), 4.73 (1H, d, J = 8.9 Hz), 4.11 (2H, t, J = 7.2 Hz), 1.85 (2H, m), 1.42–1.25 (4H, m), 1.15 (9H, s), 0.89 (3H, t, J = 7.0 Hz); ^{13}C NMR (100 MHz, CDCl₃): δ 173.5 (CO), 165.2 (CO), 136.8 (CH), 131.6 (quat.), 125.6 (quat.), 122.6 (CH), 121.8 (CH), 120.4 (CH), 110.6

(quat.), 110.4 (CH), 59.9 (CH), 47.1 (CH₂), 34.9 (quat.), 29.8 (CH₂), 29.1 (CH₂), 27.0 (CH₂), 22.4 (CH₃), 14.0 (CH₃); LRMS (+ESI): m/z 326.9 ([M - NH₃]⁺, 100%), 343.9 ([M + H]⁺, 31%); Anal. Calcd for C₂₀H₂₉N₃O₂: C, 69.94; H, 8.51; N, 12.23. Found: C, 70.23; H, 8.65; N, 12.17.

(*S*)-*N*-(1-Amino-3-methyl-1-oxobutan-2-yl)-1-(5-fluoropentyl)-1*H*-indole-3-carboxamide (5F-AB-PICA, **17**). Treating **39** (1.53 g, 6.5 mmol) with **19** (1.50 g, 9.8 mmol) according to general procedure A gave, following recrystallization from *i*-PrOH, **17** (1.56 g, 69%) as a white solid. mp 210–211 °C; 1H NMR (400 MHz, DMSO-*d*₆): δ 8.25, (1H, s), 8.11, (1H, d, J = 7.8 Hz), 7.61–7.39 (3H, m), 7.25–7.10 (2H, m), 7.07 (1H, bs), 4.47 (1H, t, J = 6.0 Hz), 4.35 (2H, m), 4.21 (2H, m), 2.09 (1H, dq, J = 13.5 Hz, 6.8 Hz), 1.84 (2H, m), 1.67 (2H, m), 1.35 (2H, m), 0.93 (6H, dd, J = 6.5 Hz, 2.9 Hz); ^{13}C NMR (100 MHz, DMSO-*d*₆): δ 173.7 (CO), 164.1 (CO), 136.1 (CH), 131.3 (quat.), 126.5 (quat.), 121.9 (CH), 121.0 (CH), 120.7 (CH), 110.4 (quat.), 109.4 (CH), 83.7 (d, $^1J_{C-F}$ = 161.7 Hz, CH₂), 57.4 (CH), 45.78 (CH₂), 30.5 (CH), 29.5 (CH₂), 29.3 (d, $^3J_{C-F}$ = 3.8 Hz, CH₂), 22.2 (d, $^2J_{C-F}$ = 5.3 Hz, CH₂), 19.5 (CH₃), 18.5 (CH₃); ^{19}F NMR (376 MHz, DMSO-*d*₆): δ -216.86; LRMS (+ESI): m/z 330.9 ([M - NH₃]⁺, 100%), 347.8 ([M + H]⁺, 67%); Anal. Calcd for C₁₉H₂₆N₃O₂F: C, 65.68; H, 7.54; N, 12.09. Found: C, 65.83; H, 7.66; N, 11.99.

(*S*)-*N*-(1-Amino-3,3-dimethyl-1-oxobutan-2-yl)-1-(5-fluoropentyl)-1*H*-indole-3-carboxamide (5F-ADBICA, **18**). Treating **39** (1.14 g, 4.9 mmol) with **20** (0.95 g, 7.3 mmol) according to general procedure A gave, following purification by flash chromatography (hexane–EtOAc, 90:10), **18** (1.14 g, 65%) as a white solid. mp 130–131 °C; 1H NMR (400 MHz, CDCl₃): δ 8.02 (1H, m), 7.71 (1H, s), 7.37 (1H, m), 7.32–7.23 (2H, m), 6.76 (1H, d, J = 9.2 Hz), 6.67 (1H, bs), 5.74 (1H, bs), 4.74 (1H, d, J = 9.2 Hz), 4.47 (2H, dt, $^2J_{H-F}$ = 48, $^3J_{H-H}$ = 6.0 Hz), 4.13 (2H, t, J = 7.1 Hz), 1.90 (2H, m), 1.70 (2H, m), 1.45 (2H, m), 1.15 (9H, s) ppm; ^{13}C NMR (100 MHz, CDCl₃): δ 173.5 (CO), 165.1 (CO), 136.7 (CH), 131.5 (quat.), 125.7 (quat.), 122.7 (CH), 121.8 (CH), 120.5 (CH), 110.8 (quat.), 110.3 (CH), 83.8 (d, $^1J_{C-F}$ = 164.8 Hz, CH₂), 59.9 (CH), 46.9 (CH₂), 34.9 (quat.), 30.1 (d, $^2J_{C-F}$ = 19.9 Hz, CH₂), 29.8 (CH₂), 27.0 (CH₃), 23.0 (d, $^3J_{C-F}$ = 5.1 Hz, CH₂); ^{19}F NMR (376 MHz, CDCl₃): δ -218.53; LRMS (+ESI): m/z 344.9 ([M - NH₃]⁺, 100%), 361.8 ([M + H]⁺, 26%); Anal. Calcd for C₂₀H₂₈N₃O₂F: C, 66.46; H, 7.81; N, 11.63. Found: C, 66.20; H, 7.94; N, 11.19.

L-*tert*-Leucinamide (**20**). To a solution of **23** (15.6 g, 59 mmol) in THF (150 mL) was added 10% Pd/C (3.0 g), and the mixture was stirred under an atmosphere of H₂ for 12 h. The suspension was filtered through a pad of Celite, and the filtrate was evaporated under reduced pressure. The resulting solid was recrystallized from EtOAc–hexane to yield **20** (4.74 g, 48%) as a white solid. mp 105–106 °C; 1H NMR (500 MHz, DMSO-*d*₆): δ 7.17 (1H, bs), 6.81 (1H, bs), 3.35 (1H, bs), 2.79 (1H, s), 1.5 (2H, bs), 0.88 (9H, s); ^{13}C NMR (125 MHz, DMSO-*d*₆): δ 176.17 (CO), 62.83 (CH), 33.56 (quat.), 26.53 (CH₃); LRMS (+ESI): m/z 130.9 ([M + H]⁺, 100%).

N-Cbz-*L*-*tert*-leucine (**22**). A cooled (0 °C) solution of *L*-*tert*-leucine (**21**, 10.0 g, 76 mmol) and 5 M aq. NaOH (15 mL, 75 mmol, 1.0 equiv) in H₂O (25 mL) was treated dropwise with benzyl chloroformate (12 mL, 84 mmol, 1.1 equiv) and 2 M aq. NaOH (42 mL, 84 mmol, 1.1 equiv), simultaneously. The mixture was warmed to rt and stirred for 2 h, and the pH was adjusted to 10 by the addition of sat. aq. NaHCO₃. The aqueous layer was washed with Et₂O (3 × 50 mL), acidified to pH 3 with 2 M aq. HCl, and extracted with Et₂O (4 × 50 mL). The combined organic phases were dried (MgSO₄), and the solvent was evaporated under reduced pressure to give a **22** (20 g, 99%) as a colorless oil. 1H NMR (400 MHz, CDCl₃): δ 7.43–7.29 (SH, m), 5.78 (1H, bs), 5.36 (1H, d, J = 9.5 Hz), 5.12 (2H, m), 4.21 (1H, d, J = 9.5 Hz), 1.02 (9H, s); ^{13}C NMR (100 MHz, CDCl₃): δ 176.0 (CO), 156.4 (CO), 136.3 (quat.), 128.7 (CH), 128.4 (CH), 128.3 (CH), 67.4 (CH), 62.3 (CH₂), 34.7 (quat.), 26.6 (CH₃); LRMS (–ESI): m/z 528.9 ([2M - H][–], 100%), 263.9 ([M - H][–], 76%).

N-Cbz-*L*-*tert*-leucinamide (**23**). To a solution of **22** (20.2 g, 76 mmol) in DMF (400 mL) were added NH₄Cl (4.95 g, 93 mmol, 1.2 equiv), Et₃N (32 mL, 229 mmol, 3.0 equiv), HOBt (13.2 g, 98 mmol,

1.3 equiv), and EDC-HCl (18.8 g, 98 mmol, 1.3 equiv). After stirring for 16 h, the reaction was quenched with sat. aq. NaHCO₃ (100 mL), and the aqueous phase was extracted with EtOAc (3 × 200 mL). The combined organic phases were washed with H₂O (3 × 200 mL) and brine (100 mL) and dried (MgSO₄), and the solvent removed under reduced pressure. The obtained crude solid was recrystallized from EtOAc–hexane to give **23** (16.9 g, 84%) as a white solid. mp 138–140 °C; ¹H NMR (300 MHz, CDCl₃): δ 7.40–7.29 (5H, m), 6.11 (1H, bs), 5.75 (1H, bs), 5.62 (1H, d, *J* = 9.5 Hz), 5.08 (2H, m), 4.03 (1H, d, *J* = 9.5 Hz), 1.01 (9H, s); ¹³C NMR (75 MHz, CDCl₃): δ 175.1 (CO), 156.7 (CO), 136.4 (quat.), 128.7 (CH), 128.3 (CH), 128.1 (CH), 67.2 (CH), 62.4 (CH₂), 34.4 (quat.), 26.6 (CH₃); LRMS (+ESI): *m/z* 264.8 ([M + H]⁺, 100%).

Methyl 1H-Indazole-3-carboxylate (25). A solution of indazole-3-carboxylic acid (**24**, 2.00 g, 12.3 mmol) in MeOH (30 mL) was treated with conc. H₂SO₄ (2 mL) and heated at reflux for 4 h. The mixture was concentrated *in vacuo* and dissolved in EtOAc (50 mL). The organic phase was washed with sat. aq. NaHCO₃ (20 mL), H₂O (20 mL), and brine (20 mL) and dried (MgSO₄), and the solvent was evaporated under reduced pressure. The crude solid was recrystallized from EtOAc–hexane to give **25** (1.65 g, 76%) as a white solid. mp 168–170 °C; ¹H NMR (300 MHz, CDCl₃): δ 8.23 (1H, m), 7.77 (1H, m), 7.49 (1H, m), 7.35 (1H, m), 4.08 (3H, s); ¹³C NMR (75 MHz, CDCl₃): δ 163.41 (CO), 141.42 (quat.), 136.27 (quat.), 127.73 (CH), 123.60 (quat.), 122.50 (CH), 121.92 (CH), 111.35 (CH), 52.31 (CH₃); LRMS (ESI): *m/z* 176.8 ([M + H]⁺, 100%).

General Procedure B: Alkylation of Methyl 1H-Indazole-3-carboxylate. To a cooled (0 °C) solution of **25** (2.17 g, 12.3 mmol) in THF (60 mL) was added *t*-BuOK (1.52 g, 13.5 mmol, 1.1 equiv). The mixture was warmed to rt, stirred for 1 h, and cooled (0 °C), and the appropriate bromoalkane (19.7 mmol, 1.6 equiv) was added dropwise. The mixture was warmed to rt and stirred for 48 h, and H₂O (60 mL) was added. The layers were separated, the aqueous layer was extracted with EtOAc (2 × 50 mL), and the combined organic phases were washed with H₂O (3 × 50 mL) and brine (20 mL) and dried (MgSO₄), and the solvent was evaporated under reduced pressure.

Methyl 1-(4-Fluorobenzyl)-1H-indazole-3-carboxylate (26). Treating **25** (2.30 g, 13.1 mmol) with 4-fluorobenzyl bromide (1.78 mL, 14.3 mmol) according to general procedure B gave, following purification by flash chromatography (hexane–EtOAc 70:30), **26** (2.50 g, 67%) as a clear glass-like solid. ¹H NMR (300 MHz, CDCl₃): δ 8.24 (1H, dt, *J* = 8.1 Hz, 1.1 Hz), 7.44–7.27 (3H, m), 7.25–7.16 (2H, m), 7.03–6.93 (2H, m), 5.67 (2H, s), 4.05 (3H, s); ¹³C NMR (75 MHz, CDCl₃): δ 163.1 (CO), 162.6 (d, ¹*J*_{C–F} = 247.3 Hz, quat.), 140.6 (quat.), 135.3 (quat.), 131.6 (d, ⁴*J*_{C–F} = 3.0 Hz, quat.), 129.2 (d, ³*J*_{C–F} = 8.1 Hz, CH), 127.3 (CH), 124.3 (CH), 123.5 (quat.), 122.5 (CH), 116.0 (d, ²*J*_{C–F} = 22.1 Hz, CH), 110.0 (CH), 53.5 (CH₂), 52.3 (CH₃); ¹⁹F NMR (282 MHz, CDCl₃): δ –113.8 (m); LRMS (+ESI): *m/z* 284.8 ([M + H]⁺, 100%).

Methyl 1-Pentyl-1H-indazole-3-carboxylate (27). Treating **25** (1.57 g, 8.9 mmol) with 1-bromopentane (1.75 mL, 14.1 mmol) according to general procedure B gave, following purification by flash chromatography (hexane–EtOAc 70:30), **27** (1.46 g, 77%) as a clear glass-like solid. ¹H NMR (400 MHz, CDCl₃): δ 8.22 (1H, m), 7.50–7.39 (2H, m), 7.30 (1H, m), 4.47 (2H, t, *J* = 7.4 Hz), 4.04 (3H, s), 1.97 (2H, quin., *J* = 7.2 Hz), 1.40–1.25 (4H, m), 0.88 (3H, m); ¹³C NMR (100 MHz, CDCl₃): δ 163.0 (CO), 140.7 (quat.), 134.9 (quat.), 126.8 (CH), 123.9 (quat.), 123.1 (CH), 122.5 (CH), 109.8 (CH), 61.1 (CH₂), 50.1 (CH₃), 29.7 (CH₂), 29.1 (CH₂), 22.4 (CH₂), 14.0 (CH₃); LRMS (+ESI): *m/z* 246.9 ([M + H]⁺, 100%).

Methyl 1-(5-Fluoropentyl)-1H-indazole-3-carboxylate (28). Treating **25** (2.30 g, 13.1 mmol) with 1-bromo-5-fluoropentane (2.42 g, 14.3 mmol) according to general procedure B gave, following purification by flash chromatography (hexane–EtOAc 70:30), **28** (2.39 g, 69%) as a colorless glass-like solid. ¹H NMR (400 MHz, CDCl₃): δ 8.24 (1H, m), 7.50–7.41 (2H, m), 7.32 (1H, m), 4.54–4.43 (3H, m), 4.35 (1H, t, *J* = 5.9 Hz), 4.04 (3H, s), 2.03 (2H, quin., *J* = 7.6 Hz), 1.80–1.64 (2H, m), 1.52–1.41 (2H, m); ¹³C NMR (100 MHz, CDCl₃): δ 163.2 (CO), 140.7 (quat.), 134.8 (quat.), 127.0 (CH), 123.9 (CH), 123.3 (quat.), 122.5 (CH), 109.7 (CH), 83.8 (d,

¹*J*_{C–F} = 165.1 Hz, quat.), 52.2 (CH₂), 49.9 (CH₃), 30.1 (d, ²*J*_{C–F} = 19.7 Hz, CH₂), 29.6 (CH₂), 22.9 (d, ³*J*_{C–F} = 5.1 Hz, CH₂); ¹⁹F NMR (376 MHz, CDCl₃): δ –218.7; LRMS (+ESI): *m/z* 264.8 ([M + H]⁺, 100%).

General Procedure C: Hydrolysis of Methyl 1-Alkyl-1H-indazole-3-carboxylates. A solution of the appropriate methyl 1-alkyl-1H-indazole-3-carboxylate (12.3 mmol) in MeOH (100 mL) was treated with 1 M aq. NaOH (18.5 mL, 18.5 mmol, 1.5 equiv) and stirred for 24 h. The solvent was reduced *in vacuo*, and the residue was dissolved in H₂O, acidified with 1 M aq. HCl, and extracted with EtOAc (2 × 50 mL). The organic phase was dried (MgSO₄), and the solvent was evaporated under reduced pressure to afford the free acid, which was used in the subsequent coupling step without further purification.

1-(4-Fluorobenzyl)-1H-indazole-3-carboxylic Acid (29). Subjecting **26** (2.30 g, 8.1 mmol) to general procedure C gave **29** (2.10 g, 96%) as a white solid. mp 200–203 °C; ¹H NMR (300 MHz, DMSO-*d*₆): δ 13.02 (1H, bs), 8.09 (1H, m), 8.47 (1H, m), 7.47 (1H, m), 7.39–7.27 (3H, m), 7.16 (2H, m), 5.76 (2H, s); ¹³C NMR (75 MHz, DMSO-*d*₆): δ 163.4 (CO), 161.7 (d, ¹*J*_{C–F} = 244.8 Hz, quat.), 140.4 (quat.), 135.1 (quat.), 132.9 (d, ⁴*J*_{C–F} = 2.8 Hz, quat.), 129.7 (d, ³*J*_{C–F} = 8.3 Hz, CH), 126.9, 123.2, 123.0, 121.6, 115.5 (d, ²*J*_{C–F} = 21.3 Hz, CH), 110.7 (CH), 51.8 (CH₂); ¹⁹F NMR (282 MHz, CDCl₃): δ –114.6; LRMS (+ESI): *m/z* 270.9 ([M + H]⁺, 100%).

1-Pentyl-1H-indazole-3-carboxylic Acid (30). Subjecting **27** (0.96 g, 3.9 mmol) to general procedure C gave **30** (0.65 g, 72%) as a white solid. mp 81–82 °C; ¹H NMR (300 MHz, CDCl₃): δ 9.85 (1H, bs), 8.26 (1H, m), 7.56–7.41 (2H, m), 7.34 (1H, m), 4.49 (2H, t, *J* = 7.3 Hz), 1.99 (2H, m), 1.45–1.25 (4H, m), 0.88 (3H, t, *J* = 6.9 Hz); ¹³C NMR (75 MHz, CDCl₃): δ 167.3 (CO), 140.9 (quat.), 134.0 (quat.), 127.0 (CH), 124.0 (quat.), 123.6 (CH), 122.5 (CH), 109.9 (CH), 50.2 (CH₂), 29.6 (CH₂), 29.0 (CH₂), 22.4 (CH₂), 14.0 (CH₃); LRMS (+ESI): *m/z* 323.9 ([M + H]⁺, 100%).

1-(5-Fluoropentyl)-1H-indazole-3-carboxylic Acid (31). Subjecting **28** (2.2 g, 8.3 mmol) to general procedure C gave **31** (1.9 g, 91%) as a white solid. mp 80–82 °C; ¹H NMR (300 MHz, CDCl₃): δ 9.88 (1H, bs), 8.27 (1H, m), 7.55–7.43 (2H, m), 7.36 (1H, m), 4.60–4.45 (3H, m), 4.34 (1H, t, *J* = 5.9 Hz), 2.06 (2H, m), 1.86–1.62 (2H, m), 1.58–1.39 (2H, m); ¹³C NMR (75 MHz, CDCl₃): δ 167.4 (CO), 140.2 (quat.), 134.2 (quat.), 127.2 (CH), 124.0 (CH), 123.7 (CH), 122.5 (quat.), 109.8 (CH), 83.8 (d, ¹*J*_{C–F} = 165.1 Hz, CH₂), 50.0 (CH₂), 30.1 (d, ²*J*_{C–F} = 19.8 Hz, CH₂), 29.5 (CH₂), 22.8 (d, ³*J*_{C–F} = 4.9 Hz, CH₂); ¹⁹F NMR (282 MHz, CDCl₃): δ –218.6; LRMS (+ESI): *m/z* 187.1 (100%), 250.9 ([M]⁺, 49%).

General Procedure D: One-Pot Synthesis of 1-Alkyl-3-(trifluoroacetyl)indoles. A cooled (0 °C) suspension of NaH (60% dispersion in mineral oil, 0.68 g, 17.1 mmol, 2.0 equiv) in DMF (10 mL) was treated with a solution of indole (**33**, 1.00 g, 8.5 mmol) in DMF (2 mL), warmed to rt, and stirred for 10 min. The mixture was cooled to 0 °C, treated slowly with the appropriate bromoalkane (1.05 equiv), warmed to rt, and stirred for 1 h. The solution was cooled to 0 °C, treated with (CF₃CO)₂O (3.00 mL, 21.3 mmol, 2.5 equiv), warmed to rt, and stirred for 1 h. The mixture was poured onto ice–water (120 mL) and stirred vigorously. The mixture was filtered, and the precipitate was dried to give the crude product as a red solid, which was used in the following step without purification.

1-(4-Fluorobenzyl)-3-(trifluoroacetyl)indole (34). Subjecting 4-fluorobenzyl bromide (1.13 mL, 9.0 mmol) to general procedure D gave **34** as a red crystalline solid (2.72 g, 100%). mp 83–86 °C; ¹H NMR (400 MHz, CDCl₃): δ 8.43 (1H, m), 7.96 (1H, m), 7.38 (1H, m), 7.43–7.29 (2H, m), 7.22–7.12 (2H, m), 7.11–7.00 (2H, m), 5.38 (2H, s); ¹³C NMR (100 MHz, CDCl₃): δ 175.1 (q, ²*J*_{C–F} = 34.9 Hz, CO), 162.9 (d, ¹*J*_{C–F} = 247.5 Hz, quat.), 137.5 (q, ³*J*_{C–F} = 4.9 Hz, CH), 136.9 (quat.), 130.7 (d, ³*J*_{C–F} = 3.4 Hz, quat.), 129.7 (d, ²*J*_{C–F} = 8.1 Hz, CH), 127.3 (quat.), 125.0 (quat.), 124.3 (CH), 123.0 (CH), 117.1 (q, ¹*J*_{C–F} = 291.8 Hz, quat.), 116.4 (d, ²*J*_{C–F} = 22.2 Hz, CH), 110.8 (CH), 110.2 (CH), 50.8 (CH₂); ¹⁹F NMR (282 MHz, CDCl₃): δ –112.9 (m), –72.3; LRMS (+ESI): *m/z* 321.9 ([M + H]⁺, 100%).

1-Pentyl-3-(trifluoroacetyl)indole (35). Subjecting 1-bromopentane (1.11 mL, 8.96 mmol) to general procedure D gave **35** as a red

crystalline solid (2.41 g, 100%). mp 56–57 °C; ^1H NMR (400 MHz, CDCl_3): δ 8.42 (1H, m), 7.93 (1H, d, $J = 1.5$ Hz), 7.47–7.33 (3H, m), 4.20 (2H, t, $J = 7.21$), 1.93 (2H, quin., $J = 7.16$ Hz), 1.46–1.31 (4H, m), 0.92 (3H, t, $J = 7.02$ Hz); ^{13}C NMR (75 MHz, CDCl_3): δ 174.9 (q, $^2J_{\text{C-F}} = 34.7$ Hz, CO), 137.4 (q, $^3J_{\text{C-F}} = 4.9$ Hz, CH), 136.8 (quat.), 127.3 (quat.), 124.6 (quat.), 124.0 (CH), 122.9 (CH), 117.3 (q, $^1J_{\text{C-F}} = 291.5$ Hz, quat.), 110.5 (CH), 109.6 (CH), 47.8 (CH_2), 29.6 (CH_2), 29.0 (CH_2), 22.3 (CH_2), 14.0 (CH_3); ^{19}F NMR (376 MHz, CDCl_3): δ -72.2; LRMS (ESI): m/z 284.0 ($[\text{M} + \text{H}]^+$, 100%).

1-(5-Fluoropentyl)-3-(trifluoroacetyl)indole (36). Subjecting 1-bromo-5-fluoropentane (1.51 g, 9.0 mmol) to general procedure D gave **36** as a red solid (2.59 g, 100%). mp 55–57 °C; ^1H NMR (500 MHz, CDCl_3): δ 8.41 (1H, m), 7.93 (1H, m), 7.46–7.32 (3H, m), 4.45 (2H, dt, $^2J_{\text{H-F}} = 45$, $^3J_{\text{H-H}} = 5.8$ Hz), 4.23 (2H, t, $J = 7.2$ Hz), 1.99 (2H, m), 1.75 (2H, m), 1.52 (2H, m); ^{13}C NMR (125 MHz, CDCl_3): δ 174.9 (q, $^2J_{\text{C-F}} = 34.8$ Hz, CO), 137.4 (q, $^3J_{\text{C-F}} = 5.0$ Hz, CH), 136.7 (quat.), 127.3 (quat.), 124.7 (CH), 124.1 (CH), 122.9 (CH), 117.2 (q, $^1J_{\text{C-F}} = 291.3$ Hz, quat.), 110.4 (CH), 109.7 (quat.), 83.7 (d, $^1J_{\text{C-F}} = 165.1$ Hz, CH_2), 47.7 (CH_2), 30.0 (d, $^2J_{\text{C-F}} = 19.9$ Hz, CH_2), 29.5 (CH_2), 23.0 (d, $^3J_{\text{C-F}} = 4.5$ Hz, CH_2); ^{19}F NMR (470 MHz, CDCl_3): δ -72.2, -218.9; LRMS (+ESI): m/z 302.0 ($[\text{M} + \text{H}]^+$, 100%).

General Procedure E: Synthesis of 1-Alkylindole-3-carboxylic Acids. To a refluxing solution of KOH (1.57 g, 28.1 mmol, 3.3 equiv) in MeOH (3 mL) was added, portionwise, a solution of the appropriate crude 1-alkyl-3-trifluoroacetylindole (8.5 mmol) in toluene (7 mL). After heating at reflux for 2 h, the mixture was cooled to ambient temperature, and H_2O (30 mL) was added. The layers were separated, and the organic layer was extracted with 1 M aq. NaOH (8 mL). The combined aqueous phases were acidified to pH 1 with 10 M aq. HCl, extracted with Et_2O (3×10 mL), and dried (MgSO_4), and the solvent was removed under reduced pressure. The crude solid was recrystallized from *i*-PrOH to give the appropriate 1-alkylindole-3-carboxylic acid as colorless crystals.

1-(4-Fluorobenzyl)indole-3-carboxylic Acid (37). Subjecting **34** (2.74 g, 8.5 mmol) to general procedure E gave **37** (1.51 g, 66%) as a colorless crystalline solid. mp 205–208 °C; ^1H NMR (400 MHz, $\text{DMSO-}d_6$): δ 8.22 (1H, s), 8.02 (1H, m), 7.54 (1H, m), 7.40–7.31 (2H, m), 7.24–7.11 (4H, m), 5.48 (2H, s); ^{13}C NMR (100 MHz, $\text{DMSO-}d_6$): δ 165.5 (CO), 161.6 (d, $^1J_{\text{C-F}} = 243.3$ Hz, quat.), 136.2 (CH), 135.4 (quat.), 133.4 (d, $^3J_{\text{C-F}} = 3.2$ Hz, quat.), 129.5 (d, $^3J_{\text{C-F}} = 8.3$ Hz, CH), 126.6 (quat.), 122.4 (CH), 121.4 (CH), 120.9 (CH), 115.4 (CH, d, $^2J_{\text{C-F}} = 21.7$), 111.0 (CH), 107.0 (quat.), 48.7 (CH_2) ppm; ^{19}F NMR (282 MHz, $\text{DMSO-}d_6$) δ -114.80 (m) ppm; LRMS (+ESI): m/z 283.9 (100%), 269.9 ($[\text{M} + \text{H}]^+$, 10%).

1-Pentylindole-3-carboxylic Acid (38). Subjecting **35** (2.00 g, 7.1 mmol) to general procedure E gave **38** (0.88 g, 54%) as a colorless crystalline solid. mp 101–102 °C (lit mp 106–108 °C); ^{13}C NMR (300 MHz, CDCl_3): δ 9.87 (1H, bs), 8.26 (1H, m), 7.93 (1H, s), 7.39 (1H, m), 7.35–7.27 (2H, m), 4.17 (2H, t, $J = 7.1$ Hz), 1.90 (2H, quin., $J = 7.1$ Hz), 1.46–1.25 (4H, m), 0.91 (3H, t, $J = 6.8$ Hz); ^{13}C NMR (75 MHz, CDCl_3): δ 170.7 (CO), 136.9 (CH), 135.6 (quat.), 127.2 (quat.), 123.0 (quat.), 122.3 (CH), 122.1 (CH), 110.2 (CH), 106.4 (CH), 47.3 (CH_2), 29.7 (CH_2), 29.1 (CH_2), 22.4 (CH_2), 14.0 (CH_3); LRMS (+ESI): m/z 245.9 (100%), 231.9 ($[\text{M} + \text{H}]^+$, 16%).

1-(5-Fluoropentyl)indol-3-carboxylic Acid (39). Subjecting **36** (2.57 g, 8.5 mmol) to general procedure E gave **39** (1.36 g, 68%) as a colorless crystalline solid. mp 117–118 °C; ^1H NMR (400 MHz, CDCl_3): δ 8.26 (1H, m), 7.93 (1H, s), 7.38 (1H, m), 7.35–7.28 (2H, m), 4.43 (2H, dt, $^2J_{\text{H-F}} = 48$, $^3J_{\text{H-H}} = 5.9$ Hz), 4.19 (2H, t, $J = 7.1$ Hz), 1.95 (2H, m), 1.73 (2H, m), 1.48 (2H, m); ^{13}C NMR (100 MHz, CDCl_3): δ 170.8 (CO), 136.8 (CH), 135.5 (quat.), 127.2 (quat.), 123.1 (CH), 122.3 (CH), 122.1 (CH), 110.1 (CH), 106.6 (quat.), 83.8 (d, $^1J_{\text{C-F}} = 164.9$ Hz, CH_2), 47.2 (CH_2), 30.1 (d, $^2J_{\text{C-F}} = 20.0$ Hz, CH_2), 29.7 (CH_2), 23.0 (d, $^3J_{\text{C-F}} = 5.0$ Hz, CH_2); ^{19}F NMR (376 MHz, CDCl_3): δ -218.6; LRMS (+ESI): m/z 263.9 (100%), 249.9 ($[\text{M} + \text{H}]^+$, 18%).

In Vitro Pharmacological Assessment of SCs. Mouse AtT-20 neuroblastoma cells stably transfected with human CB_1 or human CB_2 have been previously described^{14,36,41} and were cultured in Dulbecco's

modified Eagle's medium (DMEM) containing 10% fetal bovine serum (FBS), 100 U penicillin/streptomycin, and 300 $\mu\text{g}/\text{mL}$ G418. Cells were passaged at 80% confluence, as required. Cells for assays were grown in 75 cm^2 flasks and used at 90% confluence. The day before the assay, cells were detached from the flask with trypsin/EDTA (Sigma) and resuspended in 10 mL of Leibovitz's L-15 media supplemented with 1% FBS, 100 U penicillin/streptomycin, and 15 mM glucose (membrane potential assay and Ca^{2+} calcium assay). The cells were plated in a volume of 90 μL in black-walled, clear-bottomed 96-well microplates (Corning) that had been precoated with poly-L-lysine (Sigma, Australia). Cells were incubated overnight at 37 °C in ambient CO_2 .

Membrane potential was measured using a FLIPR membrane potential assay kit (blue) from Molecular Devices, as described previously.⁴² The dye was reconstituted with assay buffer of the following composition (mM): NaCl 145, HEPES 22, Na_2HPO_4 0.338, NaHCO_3 4.17, KH_2PO_4 0.441, MgSO_4 0.407, MgCl_2 0.493, CaCl_2 1.26, and glucose 5.56 (pH 7.4, osmolarity 315 ± 5). Prior to the assay, cells were loaded with 90 μL /well of the dye solution without removal of the L-15, giving an initial assay volume of 180 μL /well. Plates were then incubated at 37 °C at ambient CO_2 for 45 min. Fluorescence was measured using a FlexStation 3 (Molecular Devices) microplate reader, with cells excited at a wavelength of 530 nm and emission measured at 565 nm. Baseline readings were taken every 2 s for at least 2 min, at which time either drug or vehicle was added in a volume of 20 μL . The background fluorescence of cells without dye or dye without cells was negligible. Changes in fluorescence were expressed as a percentage of baseline fluorescence after subtraction of the changes produced by vehicle addition, which was less than 2% for drugs dissolved in assay buffer or DMSO. The final concentration of DMSO was not more than 0.1%.

Data were analyzed with PRISM (GraphPad Software Inc., San Diego, CA), using four-parameter nonlinear regression to fit concentration–response curves. In all plates, a maximally effective concentration of CP 55,940 was added to allow for normalization between assays.

In Vivo Pharmacological Assessment of SCs. Four cohorts of 3–4 adult male Wistar rats (Animal Resources Centre, Perth, Australia) initially weighing between 168 and 186 g were used for biotelemetry assessment of body temperature and heart rate changes following each compound or following either compound administered with a CB_1 and CB_2 antagonist. The rats were singly housed in an air-conditioned testing room (22 ± 1 °C) on a 12 h reverse light/dark cycle (lights on from 21:00 to 09:00). Standard rodent chow and water were provided *ad libitum*. All experiments were approved by The University of Sydney Animal Ethics Committee.

Biotelemetry transmitters (TA11CTA-F40, Data Sciences International, St. Paul, MN) were implanted as previously described.^{14,36} Briefly, following anesthetization (isoflurane, 3% induction, 2% maintenance), a rostro-caudal incision was made along the midline of the abdomen, and a biotelemetry transmitter (TA11CTA-F40, Data Sciences International, St. Paul, MN) was placed in the peritoneal cavity according to the manufacturer's protocol. The wound was sutured, and the rats were allowed 1 week of recovery before data collection.

The rats were habituated over multiple days to injections of vehicle (5% EtOH, 5% Tween 80, 90% physiological saline) at a set time of day (11:00 am). The first two cohorts then received injections of each compound at the same time of day in an ascending dose sequence (0.1, 0.3, 1, 3 mg/kg). This ascending sequence reduces the risk posed to the animals in assessing hitherto untested compounds, and the use of multiple cohorts limits the potential development of tolerance to the compound. Two washout days were given between each dose. If only a modest or negligible hypothermic response was seen at 3 mg/kg, then a further 10 mg/kg dose of the compound was given. At least two washout days were given between each dose.

For the antagonist studies (Figure 8), the third and fourth cohorts of drug-naïve rats were used for each compound, with a 48 h washout period between each dose. Each cohort received injections of either vehicle, CB_1 antagonist (rimonabant, 3 mg/kg), or CB_2 antagonist

(SR144528, 3 mg/kg), followed by AB-FUBINACA (3 mg/kg) or AB-PINACA (3 mg/kg). The vehicle or antagonist injections were given to rats 30 min prior to the AB-FUBINACA or AB-PINACA injection.

Data for heart rate and body temperature was gathered continuously at 1000 Hz, organized into 15 or 30 min bins using Dataquest A.R.T. software (version 4.3, Data Sciences International, St. Paul, MN), and analyzed using Prism (GraphPad Software Inc., San Diego, CA).

We calculated the area between baseline and drug-treatment body temperature curves for each rat as a measure of compound potency. Briefly, for any time point, the area between baseline data points (B_t) and drug-treatment data points (D_t) and the subsequent time points (B_{t+1} and D_{t+1}) forms a trapezoid, the area of which can be calculated via the formula

$$\text{area} = \frac{(B_t - D_t) + (B_{t+1} - D_{t+1})}{2}$$

These areas were summed from the time of injection to 6 h postinjection. This data was analyzed using a two-way mixed model ANOVA with Bonferroni corrected contrasts comparing the compounds at each dose.

For the antagonist studies, the area between the vehicle–vehicle baseline and the vehicle–SC (i.e., vehicle–AB-FUBINACA or vehicle–AB-PINACA), rimonabant–SC, and SR144528–SC treatments was calculated over a 3 h time period postinjection of SC. These areas were analyzed using a one-way repeated measures ANOVA with planned Dunnett's contrasts comparing the antagonist areas to the vehicle–drug area.

■ ASSOCIATED CONTENT

■ Supporting Information

Table of compound names, CAS numbers, and relevant references. Selected ^1H and ^{13}C NMR spectra. Additional representations of biotelemetry data. The Supporting Information is available free of charge on the ACS Publications website at DOI: 10.1021/acschemneuro.5b00112.

■ AUTHOR INFORMATION

Corresponding Author

*E-mail: michael.kassiou@sydney.edu.au.

Author Contributions

S.D.B., M.M., S.M.W., M.L., C.B., and A.S.B. performed the synthesis, purification, and chemical characterization of compounds 7–18 with guidance from M.K. J.S. conducted all *in vitro* pharmacological evaluation under the supervision of M.C., and data analysis was performed by J.S., S.D.B., and M.C. K.E.W. and R.C.K. carried out all behavioral pharmacology with direction from I.S.M. M.G. assisted the creation of stably transfected cells expressing hCB₂R. The manuscript was prepared by S.D.B., M.C., I.S.M., and M.K. All authors have given approval to the final version of the manuscript.

Funding

Work performed at The University of Sydney and presented herein was supported in part by the European Union's Seventh Framework Programme [FP7/2007-2013] INMiND (grant agreement no. HEALTH-F2-2011-278850). Work performed at Macquarie University and presented herein was supported by NHMRC project grant 1002680 awarded to M.C. and M.K.; J.S. is the recipient of an International Research Scholarship from Macquarie University

Notes

The authors declare no competing financial interest.

■ ABBREVIATIONS

ANOVA, analysis of variance; CB, cannabinoid; EDC, 1-ethyl-3-(3-dimethylaminopropyl)carbodiimide; EMCDDA, European Centre for Drugs and Drug Addiction; FLIPR, fluorometric imaging plate reader; GIRK, G protein-gated inwardly rectifying K⁺ channels; GTP γ S, guanosine 5'-O-[gamma-thio]-triphosphate; HOBt, hydroxybenzotriazole; i.p., intraperitoneal; NMR, nuclear magnetic resonance; p.i., postinjection; SAR, structure–activity relationship; SC, synthetic cannabinoid; Δ^9 -THC, Δ^9 -tetrahydrocannabinol; TLC, thin-layer chromatography

■ REFERENCES

- (1) (2015) *New Psychoactive Substances in Europe: An Update from the EU Early Warning System*, European Monitoring Centre for Drugs and Drug Addiction, Luxembourg.
- (2) Huestis, M. A., Gorelick, D. A., Heishman, S. J., Preston, K. L., Nelson, R. A., Moolchan, E. T., and Frank, R. A. (2001) Blockade of effects of smoked marijuana by the CB1-selective cannabinoid receptor antagonist SR141716. *Arch. Gen. Psychiatry* 58, 322–328.
- (3) Howlett, A. C., Barth, F., Bonner, T. I., Cabral, G., Casellas, P., Devane, W. A., Felder, C. C., Herkenham, M., Mackie, K., Martin, B. R., Mechoulam, R., and Pertwee, R. G. (2002) International Union of Pharmacology. XXVII. Classification of cannabinoid receptors. *Pharmacol. Rev.* 54, 161–202.
- (4) Pertwee, R. G., Howlett, A. C., Abood, M. E., Alexander, S. P. H., Di Marzo, V., Elphick, M. R., Greasley, P. J., Hansen, H. S., Kunos, G., Mackie, K., Mechoulam, R., and Ross, R. A. (2010) International Union of Basic and Clinical Pharmacology. LXXIX. Cannabinoid receptors and their ligands: Beyond CB1 and CB2. *Pharmacol. Rev.* 62, 588–631.
- (5) Weissman, A., Milne, G. M., and Melvin, L. S. (1982) Cannabimimetic activity from CP-47,497, a derivative of 3-phenylcyclohexanol. *J. Pharmacol. Exp. Ther.* 223, 516–523.
- (6) Wiley, J. L., Barrett, R. L., Lowe, J., Balster, R. L., and Martin, B. R. (1995) Discriminative stimulus effects of CP 55,940 and structurally dissimilar cannabinoids in rats. *Neuropharmacology* 34, 669–676.
- (7) Auwärter, V., Dresen, S., Weinmann, W., Müller, M., Putz, M., and Ferreiros, N. (2009) 'Spice' and other herbal blends: harmless incense or cannabinoid designer drugs? *J. Mass Spectrom.* 44, 832–837.
- (8) Seely, K. A., Patton, A. L., Moran, C. L., Womack, M. L., Prather, P. L., Fantegrossi, W. E., Radominska-Pandya, A., Endres, G. W., Channell, K. B., Smith, N. H., McCain, K. R., James, L. P., and Moran, J. H. (2013) Forensic investigation of K2, Spice, and "bath salt" commercial preparations: a three-year study of new designer drug products containing synthetic cannabinoid, stimulant, and hallucinogenic compounds. *Forensic Sci. Int.* 233, 416–422.
- (9) Zuba, D., and Byrska, B. (2013) Analysis of the prevalence and coexistence of synthetic cannabinoids in "herbal high" products in Poland. *Forensic Toxicol.* 31, 21–30.
- (10) Chung, H., Choi, H., Heo, S., Kim, E., and Lee, J. (2014) Synthetic cannabinoids abused in South Korea: drug identifications by the National Forensic Service from 2009 to June 2013. *Forensic Toxicol.* 32, 82–88.
- (11) Langer, N., Lindigkeit, R., Schiebel, H. M., Ernst, L., and Beuerle, T. (2014) Identification and quantification of synthetic cannabinoids in 'spice-like' herbal mixtures: a snapshot of the German situation in the autumn of 2012. *Drug Test. Anal.* 6, 59–71.
- (12) Uchiyama, N., Kawamura, M., Kikura-Hanajiri, R., and Goda, Y. (2012) Identification of two new-type synthetic cannabinoids, N-(1-adamantyl)-1-pentyl-1H-indole-3-carboxamide (APICA) and N-(1-adamantyl)-1-pentyl-1H-indazole-3-carboxamide (APINACA), and detection of five synthetic cannabinoids, AM-1220, AM-2233, AM-1241, CB-13 (CRA-13), and AM-1248, as designer drugs in illegal products. *Forensic Toxicol.* 30, 114–125.

- (13) Wilkinson, S. M., Banister, S. D., and Kassiou, M. (2015) Bioisosteric Fluorine in the Clandestine Design of Synthetic Cannabinoids. *Aust. J. Chem.* 68, 4–8.
- (14) Banister, S. D., Stuart, J., Kevin, R. C., Edington, A., Longworth, M., Wilkinson, S. M., Beinat, C., Buchanan, A. S., Hibbs, D. E., Glass, M., Connor, M., McGregor, I. S., and Kassiou, M. (2015) Effects of Bioisosteric Fluorine in Synthetic Cannabinoid Designer Drugs JWH-018, AM-2201, UR-144, XLR-11, PB-22, SF-PB-22, APICA, and STS-135. *ACS Chem. Neurosci.*, DOI: 10.1021/acschemneuro.5b00107.
- (15) Uchiyama, N., Matsuda, S., Wakana, D., Kikura-Hanajiri, R., and Goda, Y. (2013) New cannabimimetic indazole derivatives, N-(1-amino-3-methyl-1-oxobutan-2-yl)-1-pentyl-1H-indazole-3-carboxamide (AB-PINACA) and N-(1-amino-3-methyl-1-oxobutan-2-yl)-1-(4-fluorobenzyl)-1H-indazole-3-carboxamide (AB-FUBINACA) identified as designer drugs in illegal products. *Forensic Toxicol.* 31, 93–100.
- (16) Uchiyama, N., Matsuda, S., Kawamura, M., Kikura-Hanajiri, R., and Goda, Y. (2013) Two new-type cannabimimetic quinolinyl carboxylates, QUPIC and QUChIC, two new cannabimimetic carboxamide derivatives, ADB-FUBINACA and ADBICA, and five synthetic cannabinoids detected with a thiophene derivative α -PVT and an opioid receptor agonist AH-7921 identified in illegal products. *Forensic Toxicol.* 31, 223–240.
- (17) Buchler, I. P., Hayes, M. J., Hedge, S. G., Hockerman, S. L., Jones, D. E., Kortum, S. W., Rico, J. G., Tenbrink, R. E., and Wu, K. K. (2009) Indazole derivatives as CB1 receptor modulators and their preparation and use in the treatment of CB1-mediated diseases. Patent WO 2009/106982.
- (18) Centers for Disease Control and Prevention (2013) Notes from the field: Severe Illness Associated with Synthetic Cannabinoid Use — Brunswick, Georgia, 2013. *Morb. Mortal. Wkly Rep.* 62, 939.
- (19) Centers for Disease Control and Prevention (2013) Notes from the field: Severe Illness Associated with Reported Use of Synthetic Marijuana — Colorado, August–September 2013. *Morb. Mortal. Wkly Rep.* 62, 1016–1017.
- (20) Monte, A. A., Bronstein, A. C., Cao, D. J., Heard, K. J., Hoppe, J. A., Hoyte, C. O., Iwanicki, J. L., and Lavonas, E. J. (2014) An outbreak of exposure to a novel synthetic cannabinoid. *N. Engl. J. Med.* 370, 389–90.
- (21) Schwartz, M. D., Trecki, J., Edison, L. A., Steck, A. R., Arnold, J. K., and Gerona, R. R. (2015) A Common Source Outbreak of Severe Delirium Associated with Exposure to the Novel Synthetic Cannabinoid ADB-PINACA. *J. Emerg. Med.* 48, 573–580.
- (22) Uchiyama, N., Shimokawa, Y., Kawamura, M., Kikura-Hanajiri, R., and Hakamatsuka, T. (2014) Chemical analysis of a benzofuran derivative, 2-(2-ethylaminopropyl)benzofuran (2-EAPB), eight synthetic cannabinoids, five cathinone derivatives, and five other designer drugs newly detected in illegal products. *Forensic Toxicol.* 32, 266–281.
- (23) Wurita, A., Hasegawa, K., Minakata, K., Gonmori, K., Nozawa, H., Yamagishi, I., Watanabe, K., and Suzuki, O. (2015) Identification and quantitation of 5-fluoro-ADB-PINACA and MAB-CHMINACA in dubious herbal products. *Forensic Toxicol.*, DOI: 10.1007/s11419-015-0264-y.
- (24) (2014) EMCDDA–Europol 2013 Annual Report on the implementation of Council Decision 2005/387/JHA, Implementation reports, European Monitoring Centre for Drugs and Drug Addiction, Luxembourg.
- (25) Takayama, T., Suzuki, M., Todoroki, K., Inoue, K., Min, J. Z., Kikura-Hanajiri, R., Goda, Y., and Toyooka, T. (2014) UPLC/ESI-MS/MS-based determination of metabolism of several new illicit drugs, ADB-FUBINACA, AB-FUBINACA, AB-PINACA, QUPIC, SF-QUPIC and alpha-PVT, by human liver microsomes. *Biomed. Chromatogr.* 28, 831–838.
- (26) Thomsen, R., Nielsen, L. M., Holm, N. B., Rasmussen, H. B., and Linnet, K. (2014) Synthetic cannabimimetic agents metabolized by carboxylesterases. *Drug Test. Anal.*, DOI: 10.1002/dta.1731.
- (27) Wohlfarth, A., Castaneto, M. S., Zhu, M., Pang, S., Scheidweiler, K. B., Kronstrand, R., and Huestis, M. A. (2015) Pentylindole/Pentylindazole Synthetic Cannabinoids and Their 5-Fluoro Analogs Produce Different Primary Metabolites: Metabolite Profiling for AB-PINACA and SF-AB-PINACA. *AAPS J.* 17, 660–677.
- (28) Castaneto, M. S., Wohlfarth, A., Pang, S., Zhu, M., Scheidweiler, K. B., Kronstrand, R., and Huestis, M. A. (2015) Identification of AB-FUBINACA metabolites in human hepatocytes and urine using high-resolution mass spectrometry. *Forensic Toxicol.*, DOI: 10.1007/s11419-015-0275-8.
- (29) Liang, G., Choi-Sledeski, Y. M., Poli, G., Chen, X., Shum, P., Minnich, A., Wang, Q., Tsay, J., Sides, K., Cairns, J., Stoklosa, G., Nieduzak, T., Zhao, Z., Wang, J., and Vaz, R. J. (2010) A conformationally constrained inhibitor with an enhanced potency for β -tryptase and stability against semicarbazide-sensitive amine oxidase (SSAO). *Bioorg. Med. Chem. Lett.* 20, 6721–6724.
- (30) Wiley, J. L., Compton, D. R., Dai, D., Lainton, J. A. H., Phillips, M., Huffman, J. W., and Martin, B. R. (1998) Structure-activity relationships of indole- and pyrrole-derived cannabinoids. *J. Pharmacol. Exp. Ther.* 285, 995–1004.
- (31) Wiley, J. L., Marusich, J. A., and Huffman, J. W. (2014) Moving around the molecule: Relationship between chemical structure and in vivo activity of synthetic cannabinoids. *Life Sci.* 97, 55–63.
- (32) Wiley, J. L., Lefever, T. W., Cortes, R. A., and Marusich, J. A. (2014) Cross-substitution of Delta-tetrahydrocannabinol and JWH-018 in drug discrimination in rats. *Pharmacol., Biochem. Behav.* 124, 123–128.
- (33) Hine, B., Torrelío, M., and Gershon, S. (1977) Analgesic, Heart Rate, and Temperature Effects of Delta⁸-THC during Acute and Chronic Administration to Conscious Rats. *Pharmacology* 15, 65–72.
- (34) Wiley, J. L., Marusich, J. A., Martin, B. R., and Huffman, J. W. (2012) 1-Pentyl-3-phenylacetylindoles and JWH-018 share in vivo cannabinoid profiles in mice. *Drug Alcohol Depend.* 123, 148–153.
- (35) Wiley, J. L., Marusich, J. A., Lefever, T. W., Grabenauer, M., Moore, K. N., and Thomas, B. F. (2013) Cannabinoids in disguise: Delta9-tetrahydrocannabinol-like effects of tetramethylcyclopropyl ketone indoles. *Neuropharmacology* 75, 145–154.
- (36) Banister, S. D., Wilkinson, S. M., Longworth, M., Stuart, J., Apetz, N., English, K., Brooker, L., Goebel, C., Hibbs, D. E., Glass, M., Connor, M., McGregor, I. S., and Kassiou, M. (2013) The synthesis and pharmacological evaluation of adamantane-derived indoles: cannabimimetic drugs of abuse. *ACS Chem. Neurosci.* 4, 1081–1092.
- (37) Rinaldi-Carmona, M., Barth, F., Heaulme, M., Shire, D., Calandra, B., Congy, C., Martinez, S., Maruani, J., Neliat, G., Caput, D., Ferrara, P., Soubrié, P., Brelière, J. C., and Le Fura, G. (1994) SR141716A, a potent and selective antagonist of the brain cannabinoid receptor. *FEBS Lett.* 350, 240–244.
- (38) Rinaldi-Carmona, M., Barth, F., Heaulme, M., Alonso, R., Shire, D., Congy, C., Soubrié, P., Brelière, J. C., and Le Fur, G. (1995) Biochemical and pharmacological characterisation of SR141716A, the first potent and selective brain cannabinoid receptor antagonist. *Life Sci.* 56, 1941–1947.
- (39) Rinaldi-Carmona, M., Barth, F., Millan, J., Derocq, J. M., Casellas, P., Congy, C., Oustric, D., Sarran, M., Bouaboula, M., Calandra, B., Portier, M., Shire, D., Brelière, J. C., and Le Fur, G. L. (1998) SR 144528, the first potent and selective antagonist of the CB2 cannabinoid receptor. *J. Pharmacol. Exp. Ther.* 284, 644–650.
- (40) Portier, M., Rinaldi-Carmona, M., Peceue, F., Combes, T., Poinot-Chazel, C., Calandra, B., Barth, F., le Fur, G., and Casellas, P. (1999) SR 144528, an antagonist for the peripheral cannabinoid receptor that behaves as an inverse agonist. *J. Pharmacol. Exp. Ther.* 288, 582–589.
- (41) Banister, S. D., Stuart, J., Conroy, T., Longworth, M., Manohar, M., Beinat, C., Wilkinson, S. M., Kevin, R. C., Hibbs, D. E., Glass, M., Connor, M., McGregor, I. S., and Kassiou, M. (2015) Structure-activity relationships of synthetic cannabinoid designer drug RCS-4 and its regioisomers and C4 homologues. *Forensic Toxicol.*, DOI: 10.1007/s11419-015-0282-9.
- (42) Knapman, A., Santiago, M., Du, Y. P., Bennalack, P. R., Christie, M. J., and Connor, M. (2013) A continuous, fluorescence-based assay of μ -opioid receptor activation in AtT-20 cells. *J. Biomol. Screening* 18, 269–276.